HAL
open science

A Growth-Fragmentation Approach for Modeling Microtubule Dynamic Instability

Stéphane Honoré, Florence Hubert, Magali Tournus, Diana White

To cite this version:

Stéphane Honoré, Florence Hubert, Magali Tournus, Diana White. A Growth-Fragmentation Approach for Modeling Microtubule Dynamic Instability. Bulletin of Mathematical Biology, In press, 10.1007/s11538-018-0531-2 . hal-01947689

HAL Id: hal-01947689

https://hal.science/hal-01947689

Submitted on 18 Jan 2019

HAL is a multi-disciplinary open access archive for the deposit and dissemination of scientific research documents, whether they are published or not. The documents may come from teaching and research institutions in France or abroad, or from public or private research centers.

L'archive ouverte pluridisciplinaire **HAL**, est destinée au dépôt et à la diffusion de documents scientifiques de niveau recherche, publiés ou non, émanant des établissements d'enseignement et de recherche français ou étrangers, des laboratoires publics ou privés.

A growth-fragmentation approach for modeling microtubule dynamic instability

Stéphane Honoré * Florence Hubert † Magali Tournus ‡ Diana White §

Abstract

Microtubules (MTs) are protein filaments found in all eukaryotic cells which are crucial for many cellular processes including cell movement, cell differentiation, and cell division. Due to their role in cell division, they are often used as targets for chemotherapy drugs used in cancer treatment. Experimental studies of MT dynamics have played an important role in the development and administration of many novel cancer drugs, however, a complete description of MT dynamics is lacking. Here, we propose a new mathematical model for MT dynamics, that can be used to study the effects of chemotherapy drugs on MT dynamics. Our model consists of a growth-fragmentation equation describing the dynamics of a length distribution of MTs, coupled with two ODEs that describe the dynamics of free GTP- and GDP-tubulin concentrations (the individual dimers that comprise of MTs). Here, we prove the well-posedness of our system and perform a numerical exploration of the influence of certain model parameters on the systems dynamics. In particular, we focus on a qualitative description for how a certain class of destabilizing drugs, the vinca alkaloids, alter MT dynamics. Through variation of certain model parameters which we know are altered by these drugs, we make comparisons between simulation results and what is observed in *in vitro* studies.

Key-words: Growth-fragmentation model, Banach fixed point, Microtubules dynamics.
Subject Classifications: 45K05, 92C37.

1 Introduction

Microtubules (MTs) are dynamic protein polymers that are found in all eukaryotic cells. They are crucial for normal cell development, aiding in many cellular processes, including cell division, cell polarization, and cell motility [**?**]. Due to their role in cell movement and cell division, these polymers are often used as targets for a variety of cancer chemotherapy drugs. Many experimental studies have been completed to understand MT dynamics [**?**, **?**, **?**, **?**], and how these dynamics are altered by the addition of MT targeting drugs [**?**, **?**, **?**]. However, a complete understanding of such dynamics is lacking, and so the development of new theoretical models to describe MT dynamics is important.

MTs undergo a unique type of dynamics referred to as dynamic instability, which was first described by Kirschner and Mitchison in 1984 [**?**]. This type of dynamics is unique to MT polymers,

*Aix Marseille Univ, CNRS, INP, Inst Neurophysiopathol, Faculté de Pharmacie de Marseille, 13385 Marseille, France. Email: stephane.honore@univ-amu.fr, Service pharmacie, CHU Hôpital de La Timone, APHM, Marseille, France, email : stephane.honore@ap-hm.fr

†Aix Marseille Univ, CNRS, Centrale Marseille, I2M, Marseille, France. Email: florence.hubert@univ-amu.fr

‡Aix Marseille Univ, CNRS, Centrale Marseille, I2M, Marseille, France. Email: magali.tournus@centrale-marseille.fr

§Clarkson University, Department of Mathematics, Potsdam, New York. Email: dtwhite@clarkson.edu

and refers to the relative slow growth of a MT, followed by very fast depolymerization. The switch from growing to shortening is referred to as a catastrophe event, whereas the switch from shortening to growth is referred to as a rescue.

MTs are composed of tubulin heterodimers, and grow through the addition of GTP-bound tubulin (guanosine triphosphate), generally from the so called plus end of the MT, and shrink through dissociation of GDP-bound tubulin (guanosine diphosphate) at this same end [**?**]. The minus end of the MT is generally more stable, being capped by stabilizing proteins at the microtubule organizing center (MTOC).

As MTs grow, older GTP-tubulin dimers hydrolyze to the lower energy GDP tubulin, creating two distinct regions along the length of a MT. That is, a back end composed of GDP tubulin, and a front end composed of GTP tubulin. This GTP region at the growing end of a MT is referred to as the "GTP cap". Some GTP islands may persist for a long time along the GDP-microtubule lattice [**?**] [**?**]. Figure **??** shows the location of the GTP cap and GTP islands on freshly polymerized microtubules revealed by the binding of EB3 which is known to sense GTP tubulin on microtubules [**?**]. If a MT is growing at a rate faster than that of hydrolysis, the MT will continue to grow. However, if the rate of hydrolysis is greater than the rate of growth, the GTP-cap region will begin to shorten. If the cap region vanishes, the MT will undergo a so-called catastrophe, and enter a state of shortening (fragmentation). The microtubule will either depolymerize completely or it will be rescued at a GTP island. See Figure **??** for a representation of the polymerization-fragmentation-recycling cycle.

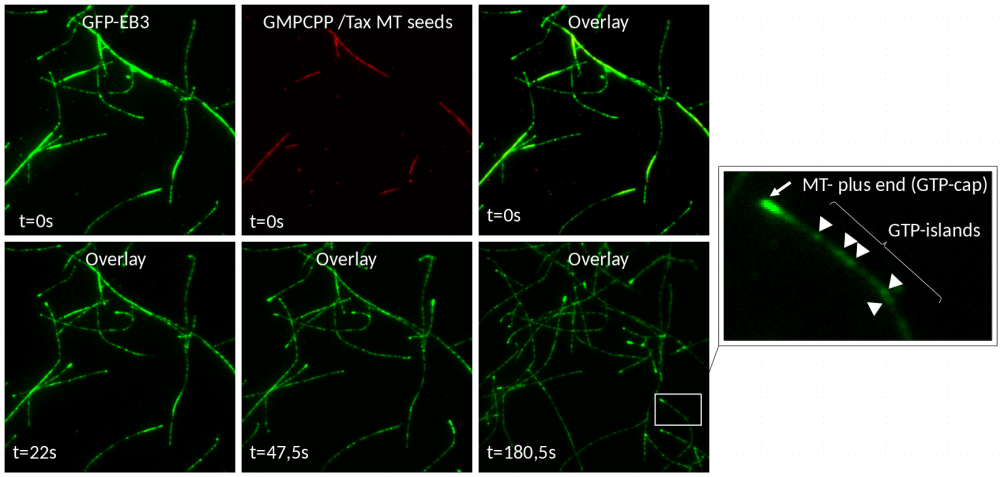

Figure 1: *In vitro* plus-end tracking assay of GFP-EB3 and measurements of MT dynamics [**?**]. The assay was performed by growing MTs in the presence of 75 nM GFP-EB3 and 15 mM brain tubulin from GMPCPP-stabilized and paclitaxel(Tax)-stabilized MT seeds. MT seeds which were immobilized on coverslips using Poly-L-Lysine PEG-biotin streptavidin links and MT polymerization was followed by TIRF microscopy of EB3-GFP fluorescence.

Since the discovery of dynamic instability, many stochastic, computational [**?**, **?**, **?**, **?**], and theoretical models [**?**, **?**, **?**] have been developed to better understand this unique type of behavior. Stochastic-type models, and many computational models provide a microscopic description of dimer addition and subtraction. In the model of Hill and Chen [**?**], a Monte Carlo simulation approach was used to describe dynamic instability at the extreme tip of a MT. The model, coined the "cap" model, refers to the fact that, above a critical concentration for tubulin, MTs exist in either one of two phases: capped (by the GTP cap) or uncapped (MT completely comprised of GDP). In the capped phase, the MT grows (with a fluctuating size in cap), and in the uncapped phase the MT quickly depolymerizes. Although this model is useful at capturing the qualitative description

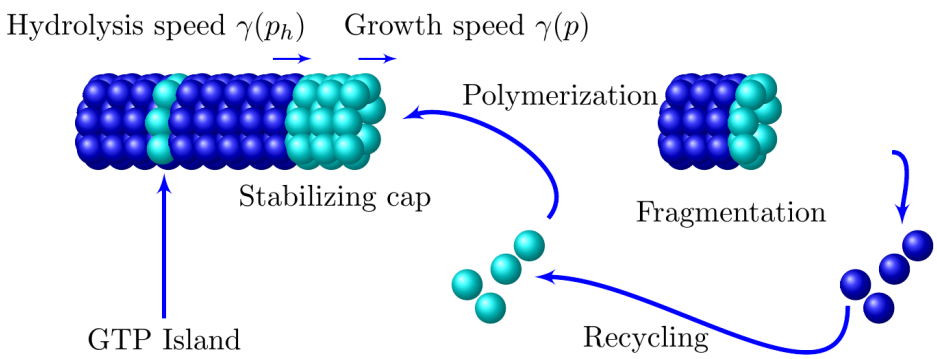

Figure 2: Schematic representation of the polymerization-fragmentation-recycling cycle. When the hydrolysis rate exceeds the growth rate, the stabilizing cap (in light blue) gradually disappears. As soon as the cap completely vanishes, a catastrophe (shortening event) can occur: the microtubule shortens and the remaining GDP tubulin (in blue) is released into the system. GDP-tubulin is then recycled into GTP tubulin (in light blue) which is used for the growth of other microtubules through polymerization.

of MT dynamic instability found in experiment, it does not give a wholly accurate quantitative description. From their simulations, Hill and Chen found a critical concentration, the concentration at which MTs begin to grow, which is about one seventh of the experimental critical concentration determined by Mitchinson and Kirschner [**?**].

Most continuous models use advection-type terms to describe MT growth and shortening at the macroscopic level. In particular, these models keep track of the lengths of growing and shortening populations of MTs over time, where the rates of both growth and shortening are either constant [**?**] or depend on the free GTP-tubulin concentration [**?**]. In the model of Dogterom and Leibler [**?**], switching between growth and shortening is described by the so called "catastrophe" and "rescue" frequencies associated with MTs. In particular, these values must be known in advance (they are model inputs) to describe MT dynamics. In the models of Hinow et al. [**?**] and White et al. [**?**], these frequencies are calculated after model simulation, which allows for a more robust examination of how these frequencies depend on MT growth dynamics.

Here, based on the Hinow model [**?**], we develop a novel deterministic modeling approach in a continuous setting to describe MT dynamics. Similar to the Hinow model, we follow the mean behavior of a family of microtubules, keeping track of MT length distributions. The uniqueness of our approach is the use of a fragmentation term in the MT dynamics equation to account for sudden MT shortening, an approach that was also used by the authors in [**?**]. This description allows for the almost "instantaneous" shortening (catastrophe) events that are often observed in MT systems. The difference between the approach described in this paper and the approach in [**?**] is that here we do not account for the MT cap length. This was accounted for in [**?**] since we were exploring the effects of end-binding proteins (EBs) on MT cap dynamics. Incorporating the MT cap makes the model considerably less tractable to prove a well posedness result, and since we are not incorporating EBs into this model, we simplify this new model by removing MT cap dynamics.

The growth-fragmentation equation is coupled to a system of ODEs that describe the dynamics of free-GTP and GDP-tubulin populations. Models consisting of an ODE coupled with an integro-partial differential equation (PDE) are already extensively used and studied in the description of Prion dynamics [**?**]. One specificity of our model is the fragmentation kernel which is not self-similar, so that our system cannot be easily reduced to a system of ODEs, like was done for Prion. Also, similar integro-PDE type models have been used by White et al. [**?**, **?**] to describe

dynamic interactions between MTs and motor proteins. In particular, these models describe MT spatial patterning, which can be driven by motor proteins whose main action is to reorient the MT network.

In addition to modeling MT dynamic instability in the base case (the case without introduction of drugs), we account for the action of MT targeting agents (MTAs) on MT dynamics through variation of certain model parameters. The two major families of drugs that are used extensively as chemotherapeutic agents are the vinca alkaloids and the taxanes [**?**, **?**]. In general, such drugs work by acting on MTs during cell division, causing cells to die [**?**, **?**, **?**]. MTA action on MTs can be very different *in vitro* and *in vivo*, and depends heavily on cellular/experimental conditions. As such, we will focus on qualitatively describing the *in vitro* action of MTAs on MT dynamics. *In vitro*, and at moderate to high doses, these drugs alter the dynamics of MTs by either promoting MT assembly/stabilization (MT stabilizing drugs like those of the taxane family) or promoting MT disassembly (MT destabilizing drugs like those from the vinca alkaloid family). At low (non-cytotoxic) doses, such drugs can alter MT dynamics without significantly altering the total MT polymer mass [**?**]. In this paper, we will primarily focus on the action of destabilizing vinblastine, as there are a number of experimental studies that describe vinblastine's role in alteration of MT dynamics [**?**, **?**].

The outline of the paper is the following: In Section **??**, we detail the development of our model which consists of an integro-partial differential equation, endowed with biologically realistic boundary conditions to describe MT dynamics, coupled with two ODEs that describe the time evolution of free GTP and GDP-tubulin concentrations. Here, we provide specific properties that certain model functions and parameters must satisfy. Section **??** is devoted to the well-posedness of the model. Here, we place more general assumptions on model parameters and functions. Finally, in Sections **??**, we perform numerical simulations to illustrate the behavior of our model in the base case. Parameters are estimated so that certain outputs of the model fit experimental data. In this section we also incorporate the action of MT targeting drugs through alteration of certain model parameters. Using these results, we explore how drugs might work to alter the normal (base case) behavior of the MT/tubulin system.

2 Description of the model

The evolution of the density $u(x,t)$ of microtubules of length $x \geq 0$ at time $t > 0$ is described by the one-dimensional growth-fragmentation equation (**??**). We neglect the complex cylindrical shape of MTs, and assume that they have linear structures.

$$\frac{\partial u(x,t)}{\partial t} + \gamma(p(t))\frac{\partial u(x,t)}{\partial x} = \beta(p(t))\left(-\int_0^x k(x,y)dy\, u(x,t) + \int_x^\infty k(y,x)u(y,t)dy\right) + N(p(t))\xi(x) \tag{1}$$

Equation (**??**) is coupled with a system of two ODEs, describing the time evolution of the concentrations of GTP-tubulin $p(t)$ and GDP-tubulin $q(t)$, respectively,

$$\frac{dp}{dt}(t) = -\gamma(p(t))\int_0^\infty u(x,t)dx - N(p(t)) + \kappa q(t), \tag{2}$$

$$\frac{dq}{dt}(t) = \beta(p(t))\int_0^\infty u(y,t)\int_0^y (y-x)k(y,x)dxdy - \kappa q(t), \tag{3}$$

endowed with initial conditions $u(x,0) = 0$, $q(0) = 0$, and $p(0) = p_0 > 0$, and with the boundary condition $u(0,t) = 0$.

Equation(**??**) describes the three main dynamic properties of MTs: nucleation, growth and shortening. The transport term of equation (**??**) describes the growth of MTs at rate $\gamma(p)$ which depends on the free GTP-tubulin concentration, since experiments suggest that MTs undergo periods of growth that are dependent on this concentration. An example of $\gamma(p)$, which is similar to growth curves found in experiment [**?**], is given by formula (**??**)

$$\gamma(p) = \begin{cases} 0 & \text{for } p < p_c \\ \alpha(p - p_c) & \text{for } p_c < p < p_\infty, \\ \alpha(p_\infty - p_c) & \text{for } p_\infty < p, \end{cases} \tag{4}$$

where p_c represents the critical concentration of tubulin required to initiate MT growth, p_∞ the saturation polymer concentration, and the growth rate parameter $\alpha > 0$.

The main novelty of the model is the assumption that depolymerization occurs instantaneously, and not at a finite rate. We assume this since MTs have been shown to shorten at rates that are orders of magnitude larger than rates of growth [**?**]. The integral term of equation (**??**) describes a shortening event. We consider that such an event has a chance to occur when the fixed rate of hydrolysis γ^h exceeds the rate of growth $\gamma(p(t))$ of a MT, where we call this value p_h. In general, when the hydrolysis rate exceeds that of growth, the MT cap shortens and a catastrophe occurs only when the cap disappears. However, if we assume that the cap is sufficiently small relative to the length of a MT, such a simplifying assumption is valid.

We assume p_∞ large enough so that $\alpha(p_\infty - p_c) > \gamma^h$, and then, $\gamma(p) < \gamma^h \Leftrightarrow p < p_h$, where we define p_h as:

$$p_h = \frac{\gamma^h + \alpha p_c}{\alpha}. \tag{5}$$

If p falls below the value p_h, MTs will have a chance to shorten. However, if p stays above the value p_h, there is no MT shortening. We introduce the parameter $\beta(p)$ defined as

$$\beta(p) = \beta_\infty(1 - H(p, p_h)), \qquad H(p, p_h) = \frac{1}{2}\left(1 + \tanh\left(\frac{p - p_h}{\varepsilon}\right)\right), \tag{6}$$

where β_∞ denotes the maximal shortening rate of MTs and $H(p, p_h)$ is a smooth approximation to a heavy-side function. Here, ε describes the steepness of the transition between 0 and β_∞ (i.e., the smaller the value of ε, the steeper the transition). The fact that the function β is smooth is a technical assumption that we need in Section **??**.

The function $k(y, x)$ from equation (**??**) represents the rescaled probability that a MT of size y shortens to a MT of size $x < y$, where the remainder of the MT completely depolymerizes into GDP-tubulin dimers. Biological observations (see Figure **??**) of such shortening events point out two different cases: either MTs of length y shorten by an average fixed length x_0 and then give rise to a newborn MT of average length $y - x_0$, or MTs of length y shorten to give rise to newborn MTs of average fixed size x_1. These two cases help define the following two shortening kernels, k_0 and k_1, respectively:

$$k_0(y, x) = G(y - x; x_0), \qquad k_1(y, x) = G(x; x_1), \quad G(z; x_*) = \frac{1}{\sigma\sqrt{2\pi}} \exp \frac{-(z - x_*)^2}{2\sigma^2}, \quad x_* > 0,\ \sigma > 0. \tag{7}$$

For simplicity, we will suppress the dependence in x_* in the notation G.

In Figure **??** (left), we show multiple kymographs from the experiment shown in Figure **??**, illustrating the dynamics of single MTs over time. A kymograph describes the growth trajectory

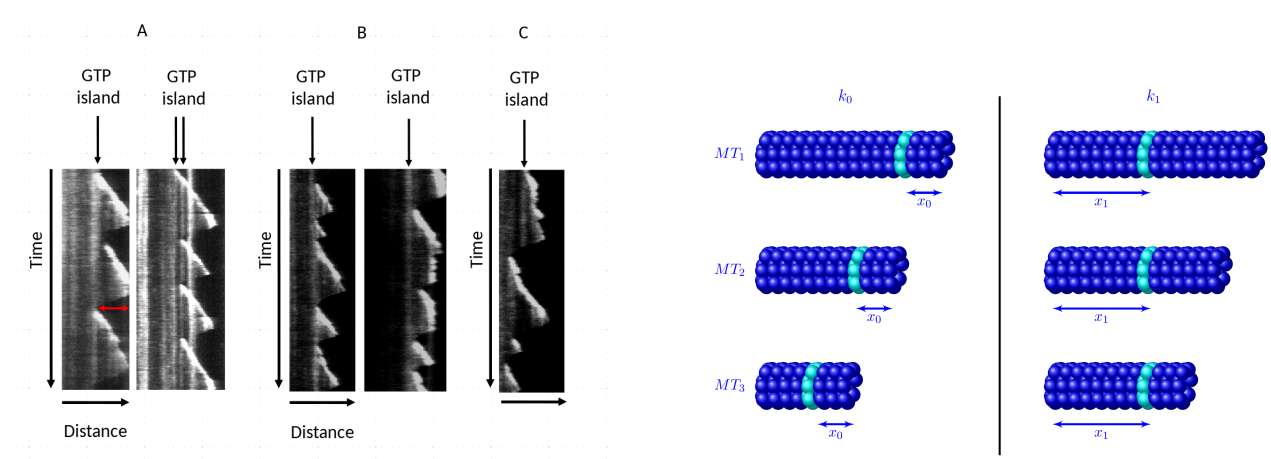

Figure 3: Examples of the growth-fragmentation process during microtubule dynamic instability. **Left**: (A) Kymographs showing a MT that shortens by approximately the same size x_0 (the appropriate kernel is k_0), (B): kymographs showing a MT that shortens to the same MT size x_1 (the appropriate kernel is k_1) represented by the most distal GTP island, (C): kymograph showing that the last distal MT island is not always a rescue site. All kymographs taken from the experiment shown in Figure **??**. **Right**: Schematic representation of the two types of kernels, k_0 and k_1, respectively.

of a single MT, and is read from top to bottom. From Figure **??**, we can observe that all MTs shorten by approximately the same distance x_0, or toward a stable part of the MT lattice (i.e., the MT seed or GTP island). Thus, the shortening kernels k_0 and k_1 may represent most cases, even if the reality may be more complex. Here, the shortening distances can be fit to a Gaussian like k_0, where the standard deviation σ is very small. Possible values for x_0 and its standard deviation σ are summarized in Table **??**.

The final source term in equation (**??**), $N(p)$, describes MT nucleation (the birth of a MT). We assume

$$N(p) = \mu p^m H(p, p_N), \tag{8}$$

where $H(p, p_N)$ is defined as in equation (**??**). In particular, equation (**??**) states that if the value for GTP-tubulin (p) falls below the critical nucleation value p_N, nucleation is *switched off*. Here, μ is called the nucleation parameter and m is linked to the minimum number of GTP-tubulin dimers required for nucleation. Freshly nucleated MTs have a size between 0 and x_{min}. The weight $\xi(x)$ is then defined as

$$\xi(x) = C_N(1 - H(x, x_{min})). \tag{9}$$

Here x_{min} is defined in Table **??** and C_N is a normalization constant that ensures we have the property

$$\int_0^\infty \xi(x)\, x dx = 1. \tag{10}$$

Equations (**??**) and (**??**) represent the time evolution of GTP and GDP-tubulin, respectively. The first term in equation (**??**) describes a decrease of GTP tubulin due to MT growth, while the second term describes a decrease due to nucleation. The final term describes GDP/GTP recycling, where $\kappa > 0$ is the recycling rate of GDP to GTP. The first term in equation (**??**) describes all

GDP-tubulin which comes from a shortening event, while the second term accounts for GDP/GTP recycling.

It can be shown by formal integration that the total mass of the system (**??**),(**??**), (**??**) is preserved. Specifically, the total amount of tubulin in polymer and free form does not vary with time so that

$$\frac{d}{dt}\left(\int_0^\infty xu(x,t)dx + p(t) + q(t)\right) = 0.$$

It can also be shown that increase in the total number of MTs is only due to nucleation. That is,

$$\frac{d}{dt}\left(\int_0^\infty u(x,t)dx\right) = N(p(t))\int_0^\infty \xi(x)dx.$$

3 Well posedness of the PDE model

In this section of the paper, we focus on the well-posedness of the model developed in Section **??**. To avoid cumbersome calculations, we reduce the system defined by equations (**??**), (**??**), and (**??**) to a system of two equations. In particular, we assume that the exchange rate of GDP-tubulin to GTP-tubulin is instantaneous (assumption that is reasonable in vitro in excess of GTP or in cells in absence of alteration of ATP-production), and so we need only to consider the equations for u and p. The generalization of the results that follow, to the full system, is straightforward. The PDE model we consider is written as

$$\frac{\partial u(x,t)}{\partial t} + \gamma(p(t))\frac{\partial u(x,t)}{\partial x} = \beta(p(t))\left(-\int_0^x k(x,y)dy\, u(x,t) + \int_x^\infty k(y,x)u(y,t)dy\right) + N(p(t))\xi(x), \tag{11}$$

$$\frac{dp}{dt}(t) = -\gamma(p(t))\int_0^\infty u(x,t)dx + \beta(p(t))\int_0^\infty u(y,t)\int_0^y (y-x)k(y,x)dxdy - N(p(t)), \tag{12}$$

$$u(x,0) = 0, \quad u(0,t) = 0, \quad p(0) = p_0. \tag{13}$$

A similar system was introduced and developed in the context of Prion proliferation. Global existence and uniqueness of a global solution was then studied in [**?**, **?**, **?**] using semi-group theory. The main difference between our model and that studied in [**?**] and [**?**] are the time-dependence of the function β and the fact that the fragmentation kernel is not self-similar.

3.1 Assumptions on the parameters

Here, we outline assumptions on model parameters required for our main result. The polymerization growth rate $\gamma(p)$ is Lipschitz and bounded so that

$$0 \le \gamma(p_1) \le \gamma_\infty, \qquad |\gamma(p_1) - \gamma(p_2)| \le \alpha|p_1 - p_2|, \quad p_1, p_2 \in \mathbb{R}^+. \tag{14}$$

The nucleation density satisfies

$$\xi \in C^1(\mathbb{R}^+), \quad \int_0^\infty \xi(x)\, xdx = 1, \quad Supp(\xi) \subset [x_m^\xi, x_M^\xi], \quad I_\xi := \int_0^\infty \xi(x)\, dx < \infty, \tag{15}$$

$$0 \le N(p) \le N_\infty, \quad p \in \mathbb{R}^+. \tag{16}$$

The rate of fragmentation satisfies

$$\beta \in L^\infty(\mathbb{R}^+) \cap C^1(\mathbb{R}^+), \quad 0 \le \beta(p) \le \beta_\infty, \quad p \in \mathbb{R}^+. \tag{17}$$

All parameters satisfy $\gamma(p) = N(p) = \beta(p) = 0$ for $p < 0$. The fragmentation rate is bounded such that

$$\int_0^y k(y,x)dx = B(y), \quad B \in L^\infty(\mathbb{R}^+), \tag{18}$$

where the kernel k satisfies

$$k(x,x) = 0,\ x \in \mathbb{R}^+, \quad k(x,0) = 0,\ x \in \mathbb{R}^+, \quad k(x,y) = 0 \text{ if } x < y, \quad x,y \in \mathbb{R}^+, \tag{19}$$

and we assume the additional properties

$$\int_0^y k(y,x)(y-x)dx \le M_0 + M_1 y, \quad \int_0^y |\partial_1 k(y,x)|\, dx \le M_2, \quad \int_0^y |\partial_2 k(y,x)|\, dx \le M_3. \tag{20}$$

Two different kernels are considered for application:

$$k_0(y,x) = \begin{cases} G_0(y-x), & y > x, \\ 0, & \text{otherwise}, \end{cases} \qquad k_1(y,x) = \begin{cases} G_1(x), & y > x, \\ 0, & \text{otherwise}, \end{cases} \tag{21}$$

for some $G_0, G_1 \in \mathcal{C}^1_C(0,+\infty)$. These two kernels correspond to the experimentally observed cases illustrated in Figure **??**. The kernel k_0 satisfies properties (**??**) with $M_1 = 0$. In the case $M_1 = 0$, the proof of existence is easier (than when $M_1 \neq 0$), thus we treat this case independently. For any $f \in L^\infty(\mathbb{R}^+)$ we use the notation $f_\infty := \|f\|_{L^\infty(\mathbb{R}^+)}$.

3.2 Main result

A weak solution of to the system (**??**) (**??**) is defined as a couple $(u,p) \in C(\mathbb{R}^+; L^1(\mathbb{R}^+, (1+x)dx)) \times C(\mathbb{R}^+)$ such that (**??**) (**??**) is satisfied in the sense of distributions.

Theorem 1. *Under assumptions* (**??**), (**??**), (**??**), (**??**), (**??**) (**??**) *and* (**??**) *, there exists a unique weak solution* $(u,p) \in C(\mathbb{R}^+; L^1(\mathbb{R}^+, (1+x)dx)) \times C(\mathbb{R}^+)$ *to the system* (**??**) (**??**)*. Moreover it satisfies for all* $T \ge 0$

$$0 \le p(T) \le p_0, \qquad \int_{\mathbb{R}^+} u(x,T)x dx \le p_0, \quad \textit{and} \quad \int_{\mathbb{R}^+} u(x,T)dx \le N(p_0)T,$$

$$\textit{and} \quad \int_{\mathbb{R}^+} \left|\frac{\partial u}{\partial x}(x,T)\right| dx \le K_1 T + K_2 T^2,$$

for some positive constants K_1 *and* K_2 *given by*

$$K_1 = (x_M^\xi - x_m^\xi) N(p_0) \xi'_\infty, \quad K_2 = \frac{\beta(p_0)}{2} N(p_0) I_\xi (M_2 + M_3).$$

Strategy of the proof We build a sequence $T_0, T_1, T_2 \dots$ and prove by induction that the system (**??**) (**??**) admits a unique solution over $[0, T_n]$, and that $T_n \to \infty$. To do so, we assume that there exists a unique solution (u^*, p^*) to the system (**??**), (**??**) over $[0, T_n]$. To extend this solution to $[T_n, T_{n+1}]$, we use the Banach fixed point theorem in the Banach space $Y = C([T_n, T])$ endowed with $\|p\|_Y = \sup_{T_n \le t \le T} \|p(t)\|$. For a given function $\bar{p} \in Y$, we define u as the unique solution for $t \ge T_n$ and $x \ge 0$ to the equation

$$\frac{\partial u(x,t)}{\partial t} + \gamma(\bar{p}(t)) \frac{\partial u(x,t)}{\partial x} = \beta(\bar{p}(t)) \left(-u(x,t) \int_0^x k(x,y)dy + \int_x^\infty k(y,x)u(y,t)dy \right) + N(\bar{p}(t))\xi(x), \tag{22}$$

$$u(x,T_n) = u^*(x,T_n), \quad u(0,t) = 0. \tag{23}$$

For the function u given by equations (**??**) and (**??**), we then define $p := \mathbf{G}[\bar{p}]$ as the unique solution satisfying the equation

$$\frac{dp}{dt}(t) = -\gamma(\bar{p}(t)) \int_0^\infty u(x,t)dx + \beta(\bar{p}(t)) \int_0^\infty u(y,t) \int_0^y (y-x)k(y,x)dxdy - N(\bar{p}(t)) \tag{24}$$

$$p(T_n) = p^*(T_n), \tag{25}$$

for $t \geq T_n$ and $x \geq 0$.

We obtain the unique extent (u,p) to the solution (u^*,p^*) of system (**??**) and (**??**), over $[T_n, T_{n+1}]$ as the unique fixed point to map $\mathbf{G}$ for p, and the unique u satisfying (**??**) and (**??**) where we replaced $\bar{p}$ by p. To make further notation less complicated, we drop the dependence in n for the space Y and the map $\mathbf{G}$. The sequence of lemmas that follow provide us with the necessary details needed to extend the solution to $[T_n, T_{n+1}]$, and provides us with an explicit expression for T_{n+1}. These steps will lead us to the desired end result, the proof of Theorem **??**. As a first step, we show that $\mathbf{G}$ is well defined.

3.3 The transport-fragmentation equation

For $a, b, c \in L^\infty(\mathbb{R}^+)$ and $T_n > 0$ given, we consider the transport-fragmentation equation for $x \geq 0$ and $t \geq T_n$

$$\begin{cases} \dfrac{\partial u(x,t)}{\partial t} + a(t)\dfrac{\partial u(x,t)}{\partial x} = b(t)\left(-u(x,t)\displaystyle\int_0^x k(x,y)dy + \int_x^\infty k(y,x)u(y,t)dy\right) + c(t)\xi(x), \\ u(x,T_n) = u^*(x,T_n), \quad x \geq 0, \qquad u(0,t) = 0, \quad t \geq T_n. \end{cases} \tag{26}$$

Lemma 1 (Well posedness of (**??**))**.** *Assume $a, b, c \in L^\infty(\mathbb{R}^+)$ with $a \geq 0,\ b \geq 0,\ c \geq 0$, then, there exists a unique solution to (**??**) in $\mathcal{C}([T_n,\infty), L^1(\mathbb{R}^+))$. Moreover, we have the following properties*

1. *Positivity. If $u^*(.,T_n) \geq 0$, then $u(.,t) \geq 0$ for $t \geq T_n$.*
2. *Compact support. If for some $M > x_M^\xi$, $supp(u^*(.,T_n)) \subset [0, M + a_\infty T_n]$ (this is true for $T_n = 0$), then $supp(u(.,t)) \subset [0, M + a_\infty t]$ for $t \geq T_n$.*

Proof. The proof of Lemma **??** relies on a (second) fixed point argument. For any $\bar{u} \in C(\mathbb{R}^+, L^1(\mathbb{R}^+))$ such that $\bar{u} \geq 0$, *a.e.*, we define $u := \mathbf{F}[\bar{u}]$ as the unique distributional solution $u \in C(\mathbb{R}^+; L^1(\mathbb{R}^+))$ to

$$\begin{cases} \dfrac{\partial u(x,t)}{\partial t} + a(t)\dfrac{\partial u(x,t)}{\partial x} = b(t)\left(-B(x)u(x,t) + \displaystyle\int_x^\infty k(y,x)\bar{u}(y,t)dy\right) + c(t)\xi(x), \\ u(x,T_n) = u^*(x,T_n), \quad x \geq 0, \qquad u(0,t) = 0, \quad t \geq T_n. \end{cases} \tag{27}$$

Step 1. The map F is well defined.

Based on the method of characteristics, we explain why the map $\mathbf{F}$ is well defined. The characteristic curves are defined for all time $t \geq T_n$ as

$$\dot{Z}(t;t_0,y_0) = a(t), \qquad Z(t_0;t_0,y_0) = y_0,$$

and for all $(x,t) \in \mathbb{R}^+ \times [T_n, +\infty)$, there exists a unique (x_0, t_0) such that either $t_0 = T_n$, either $x = 0$ and such that $Z(t; t_0, x_0) = x$. Let us first assume $\bar{u} \in \mathcal{C}^1(\mathbb{R}^+ \times \mathbb{R}^+)$ and $u^*(., T_n) \in \mathcal{C}^1(\mathbb{R}^+)$. The function u is a solution to (**??**) if and only if it satisfies the linear equation

$$\begin{aligned}\frac{d}{dt}u(Z(t;t_0,y_0),t) =& b(t)\left(-B(Z(t;t_0,y_0))u(Z(t;t_0,y_0),t) + \int_{Z(t;t_0,y_0)}^{\infty} k(y, Z(t;t_0,y_0))\bar{u}(y,t)dy\right) \\ &+ c(t)\,\xi(Z(t;t_0,y_0)).\end{aligned} \tag{28}$$

There exists a unique global solution $u(Z(t;t_0,y_0),t))$ to the linear ODE (**??**) since b, B, k, c and ξ are continuous and nonnegative. A regularization process (i.e. we approximate u^* and $\bar{u}$ by a sequence of C^1 functions u_k^* and $\bar{u}_k$) gives us the existence of a weak solution $u \in \mathcal{C}^1(\mathbb{R}^+, L^1(\mathbb{R}^+))$ for $\bar{u} \in \mathcal{C}^1(\mathbb{R}^+, L^1(\mathbb{R}^+))$ and $u^*(., T_n) \in L^1(\mathbb{R}^+)$. Uniqueness of u is clear since the difference of two solutions satisfies a linear transport equation with linear source term. Moreover, we have $u(x,t) \geq 0$, *a.e.* **Step 2. The solution u is compactly supported.** Let us assume $\text{supp}(u^*(., T_n)) \subset [0, M + a_\infty T_n]$ and $\text{supp}(\bar{u}(., t)) \subset [0, M + a_\infty t]$ for $t \geq T_n$ for some $M > x_M^\xi$. The characteristic curve passing through a point (x,t) where $x > M + a_\infty t$ emanates from (x, T_n) where $x > M + a_\infty T_n$ (or from $(0, t_0)$ for a given $t_0 \geq 0$). On the characteristic curves emanating from the anchors (x, T_n) where $x \geq M + a_\infty T_n \geq x_M^\xi$, the solution u is constantly equal to zero (both the initial condition and source term are zero) . Then, for $x > M + a_\infty t$, with $M > x_M^\xi$, we have $u(x,t) = 0$.
Step 3. The map F is a contraction. We prove here that **F** is a contractive map in the Banach space

$$X = C^+([T_n, T_n + T]; L^1(\mathbb{R}^+, dx)), \qquad \|u\|_X = \sup_{T_n \leq t \leq T_n + T} \|u(t,.)\|_{L^1(\mathbb{R}^+,\, dx)}.$$

The proof is a straightforward adaptation from [**?**], page 59. For $(\bar{u}_1, \bar{u}_2) \in X^2$, we define $(u_1, u_2) \in X^2$ as $u_1 := \mathbf{F}[\bar{u}_1]$ and $u_2 := \mathbf{F}[\bar{u}_2]$. The function $u = u_1 - u_2$ then satisfies for $\bar{u} = \bar{u}_1 - \bar{u}_2$

$$\frac{\partial u(x,t)}{\partial t} + a(t)\frac{\partial u(x,t)}{\partial x} = b(t)\left(-B(x)u(x,t) + \int_x^\infty k(y,x)\bar{u}(y,t)dy\right).$$

We multiply the above equation by $\text{sign}(u)$, integrate over $\mathbb{R}^+$, and intergrate with time to get

$$\|u\|_X \leq T\, b_\infty B_\infty \|\bar{u}\|_X,$$

which means that as soon as $T < 1/(2b_\infty B_\infty)$, **F** is a strict contraction in the Banach space X and this proves the existence of a unique fixed point. We can iterate the operator on $[T_n + T, T_n + 2T], [T_n + 2T, T_n + 3T], \ldots$. since the condition on T does not depend on the iteration. With this iteration process, we have built a solution to (**??**) in $\mathcal{C}^+([T_n, +\infty), L^1(\mathbb{R}^+))$. Properties 1 and 2 of Lemma **??** are preserved by the map **F** and are thus true for the fixed point.

□

The intermediate estimates stated in Lemma **??** to **??** are useful to prove that the map **G** is a contraction from Y to Y.

Lemma 2 (L^1-estimate)**.** *Assume $a, b, c \in L^\infty(\mathbb{R}^+)$. The solution to* (**??**) *satisfies for $A_1 = c_\infty I_\xi$*

$$\int_{\mathbb{R}^+} u^*(x, T_n)dx \leq A_1 T_n \quad \textit{implies} \quad \int_{\mathbb{R}^+} u(x,t)dx \leq A_1 t, \quad t \geq T_n.$$

Proof. We integrate equation (**??**) over $\mathbb{R}^+$ and use the condition at $x = 0$ and the compact support property

$$\frac{d}{dt}\int_{\mathbb{R}^+} u(x,t)dx = c(t)I_\xi \le c_\infty I_\xi, \quad t \ge T_n,$$

which directly implies Lemma **??** after a time integration. □

Lemma 3 ($W^{1,1}$ estimate)**.** *Assume $a, b, c \in L^\infty(\mathbb{R}^+)$. Then there are some positive constants A_2 and A_3 such that if u^* satisfies the premise of Lemma **??**, then the solution to (**??**) satisfies for $t \ge T_n$*

$$\int_{\mathbb{R}^+}\left|\frac{\partial u^*}{\partial x}\right|(x,T_n)dx \le A_2T_n^2 + A_3T_n \quad \textit{implies} \quad \int_{\mathbb{R}^+}\left|\frac{\partial u}{\partial x}\right|(x,t)dx \le A_2t^2 + A_3t,$$

with

$$A_2 = \frac{1}{2}b_\infty c_\infty I_\xi(M_2 + M_3), \quad A_3 = (x_M^\xi - x_m^\xi)c_\infty \xi'_\infty.$$

Proof. Let us first differentiate equation (**??**) with respect to x (on a regularized solution):

$$\begin{aligned}\frac{\partial}{\partial t}\frac{\partial u}{\partial x}(x,t) + a(t)\frac{\partial}{\partial x}\frac{\partial u}{\partial x}(x,t) =& b(t)\Big(-u(x,t)\frac{\partial}{\partial x}\int_0^x k(x,y)dy - B(x)\frac{\partial u}{\partial x}(x,t)\\ &+ \frac{\partial}{\partial x}\int_x^\infty k(y,x)u(y,t)dy\Big) + c(t)\frac{\partial \xi}{\partial x}(x).\end{aligned} \tag{29}$$

We notice that, thanks to (**??**) (**??**)

$$\frac{\partial}{\partial x}\int_0^x k(x,y)dy = \int_0^x \partial_1 k(y,x)dy, \quad \frac{\partial}{\partial x}\int_x^\infty k(y,x)u(y,t)dy \quad = \int_x^\infty \partial_2 k(y,x)u(y,t)dy,$$

since $k(x,x) = 0$. We now formally multiply (**??**) by $\operatorname{sign}\left(\frac{\partial u}{\partial x}(x,t)\right)$ (actually, we multiply by a regularization of $\operatorname{sign}\left(\frac{\partial u}{\partial x}(x,t)\right)$ and pass to the limit - see section 3.4 of [**?**] for details). From this, we get

$$\begin{aligned}&\frac{\partial}{\partial t}\left|\frac{\partial u}{\partial x}\right|(x,t) + a(t)\frac{\partial}{\partial x}\left|\frac{\partial u}{\partial x}\right|(x,t) = b(t)\Big(-B(x)\left|\frac{\partial u}{\partial x}(x,t)\right| - \operatorname{sign}\left(\frac{\partial u}{\partial x}(x,t)\right)u(x,t)\int_0^x \partial_1 k(y,x)dy\\ &+ \int_x^\infty \operatorname{sign}\left(\frac{\partial u}{\partial x}(x,t)\right)\partial_2 k(y,x)u(y,t)dy\Big) + c(t)\operatorname{sign}\left(\frac{\partial u}{\partial x}(x,t)\right)\frac{\partial \xi}{\partial x}(x).\end{aligned}$$

And, after integration we have

$$\frac{d}{dt}\int_{\mathbb{R}^+}\left|\frac{\partial u}{\partial x}(x,t)\right|dx \le F_1(t) + F_2(t) + F_3(t) + F_4(t) + F_5(t),$$

where, using Lemma **??** for F_3 and F_5,

$$F_2(t) = -b(t)\int_{\mathbb{R}^+} B(x)\left|\frac{\partial u}{\partial x}(x,t)\right|dx \le 0,$$

$$F_3(t) \le b(t)\int_{\mathbb{R}^+}\int_0^x |\partial_1 k(y,x)||u(x,t)|dydx \le b_\infty M_2 c_\infty I_\xi t,$$

$$F_5(t) \leq b(t) \int_{\mathbb{R}^+} \int_x^\infty |\partial_2 k(y,x)||u(y,t)| dy dx \leq b_\infty c_\infty I_\xi M_3 t$$

$$F_6(t) = c(t) \int_{\mathbb{R}^+} \left| \frac{\partial \xi}{\partial x}(x) \right| dx \leq c_\infty (x_M^\xi - x_m^\xi) \xi'_\infty,$$

and since $u(0,t) = 0$, writing equation (**??**) at $x = 0$ gives us

$$F_1(t) = -a(t) \left| \frac{\partial u}{\partial x}(0,t) \right| = b(t) \int_0^\infty k(y,0) u(y,t) dy + c(t)\xi(0) = 0.$$

In summary, we have

$$\frac{d}{dt} \int_{\mathbb{R}^+} \left| \frac{\partial u}{\partial x}(x,t) \right| dx \leq b_\infty c_\infty I_\xi \left(M2 + M3 \right) t + c_\infty (x_M^\xi - x_m^\xi) \xi'_\infty,$$

Then, integrating over $[T_n, t]$ we obtain the conclusion of Lemma **??**.

□

Lemma 4 (L^1-stability)**.** *For (a_1, b_1, c_1) and (a_2, b_2, c_2) two triplets of functions of $L^\infty(\mathbb{R}^+)$, if u_2^* satisfies the premise of Lemma* **??** *and Lemma* **??**, *the associated solutions u_1 and u_2 to* (**??**) *satisfy for $t \geq T_n$*

$$\int_{\mathbb{R}^+} |u(x,t)| dx \leq A_4 \|a_1 - a_2\|_\infty t^3 + \left(A_3 \|a_1 - a_2\|_\infty + A_5 \|b_1 - b_2\|_\infty \right) t^2 + I_\xi \|c_1 - c_2\|_\infty t$$

where

$$u = u_1 - u_2, \quad A_4 = \frac{A_2}{3}, \quad A_5 = 2B_\infty c_\infty I_\xi.$$

Proof. The difference u satisfies

$$\begin{aligned}
\frac{\partial u}{\partial t}(x,t) = -a_1(t) \frac{\partial u}{\partial x}(x,t) &+ (a_2(t) - a_1(t)) \frac{\partial u_2}{\partial x}(x,t) \\
&+ b_1(t) \left(-B(x) u(x,t) + \int_x^\infty k(y,x) u(y,t) dy \right) \\
&+ (b_1(t) - b_2(t)) \left(B(x) u_2(x,t) - \int_x^\infty k(y,x) u_2(y,t) dy \right) \\
&+ (c_1(t) - c_2(t)) \xi(x).
\end{aligned}$$

Multiplying by $\text{sign}(u(x,t))$ we obtain

$$\begin{aligned}
\frac{\partial |u|}{\partial t}(x,t) \leq &- a_1(t) \frac{\partial |u|}{\partial x}(x,t) + |a_2(t) - a_1(t)| \left| \frac{\partial u_2}{\partial x}(x,t) \right| \\
&+ b_1(t) \left(-B(x)|u(x,t)| + \int_x^\infty k(y,x)|u(y,t)| dy \right) \\
&+ |b_1(t) - b_2(t)| \left(B(x)|u_2(x,t)| + \int_x^\infty k(y,x)|u_2(y,t)| dy \right) \\
&+ |c_1(t) - c_2(t)| \xi(x).
\end{aligned}$$

Now, we integrate over $\mathbb{R}^+$ and get

$$\begin{aligned}
\frac{d}{dt} \int_{\mathbb{R}^+} |u(x,t)| dx \leq &|a_2(t) - a_1(t)| \int_0^\infty \left| \frac{\partial u_2}{\partial x}(x,t) \right| dx + |c_1(t) - c_2(t)| I_\xi \\
&+ |b_1(t) - b_2(t)| \left(\int_0^\infty B(x)|u_2(x,t)| dx + \int_0^\infty \int_x^\infty k(y,x)|u_2(y,t)| dy dx \right),
\end{aligned}$$

and so

$$\frac{d}{dt}\int_{\mathbb{R}^+}|u(x,t)|dx \leq \|a_1-a_2\|_\infty(A_2t^2+A_3t)+I_\xi\|c_1-c_2\|_\infty+2\|b_1-b_2\|_\infty B_\infty c_\infty I_\xi t.$$

Integrating over time and taking the supremum over $t\in[T_n,t]$, we arrive at the conclusion of Lemma **??**. □

Lemma 5 ($L^1(xdx)$ estimate - only for $M_1\neq 0$)**.** *Assume $a,b,c\in L^\infty(\mathbb{R}^+)$. Then, if u^* satisfies the premise of Lemma* **??**, *the solution u to* (**??**) *satisfies*

$$\int_{\mathbb{R}^+}u^*(x,T_n)xdx\leq p_0 \quad \textit{implies} \quad \int_{\mathbb{R}^+}u(x,t)xdx\leq A_6e^{A_7(t-T_n)}+A_6'T_ne^{A_7(t-T_n)},\quad t\geq T_n$$

with

$$A_6=p_0+\frac{c_\infty(b_\infty M_1+I_\xi a_\infty+b_\infty M_0I_\xi)}{b_\infty^2M_1^2},\quad A_6'=\frac{c_\infty I_\xi(b_\infty M_0+a_\infty)}{b_\infty M_1},\quad A_7=b_\infty M_1.$$

Proof. We multiply equation (**??**) by x and integrate over $\mathbb{R}^+$ to get

$$\frac{d}{dt}\int_{R^+}xu(x,t)dx=a(t)\int_{\mathbb{R}^+}u(x,t)dx+c(t)+b(t)\int_{\mathbb{R}^+}\int_0^y k(y,x)(x-y)u(y,t)dxdy$$

which implies

$$\frac{d}{dt}\int_{\mathbb{R}^+}xu(x,t)dx\leq a_\infty c_\infty I_\xi t+c_\infty+b_\infty\left(M_0c_\infty I_\xi t+M_1\int_{\mathbb{R}^+}xu(x,t)dx\right).$$

The solutions to the ODE $g'(t)=r+st+wg(t)$ are written

$$g_C(t)=Ce^{wt}-\frac{rw+1}{w^2}-\frac{s}{w}t,$$

then, the solutions f to

$$f'(t)\leq r+st+wf(t),\qquad f(T_n)\leq p_0,$$

satisfy for any $C\in\mathbb{R}$ (Gronwall Lemma)

$$f(t)\leq g_C(t)+(f(T_n)-g_C(T_n))e^{w(t-T_n)}.$$

Thus, if we take C such as $g_C(T_n)=p_0$, i.e. $C=\left(p_0+\frac{rw+s}{w^2}\right)e^{-wT_n}+\frac{s}{w}T_ne^{-wT_n}$ we have $f(t)\leq Ce^{wt}$, which leads to Lemma **??**. □

Lemma 6 ($W^{1,1}(xdx)$ estimate - only for $M_1\neq 0$)**.** *Assume $a,b,c\in L^\infty(\mathbb{R}^+)$. If u^* satisfies the premise of Lemma* **??** *and Lemma* **??**, *and if*

$$\int_{\mathbb{R}^+}\left|\frac{\partial u^*}{\partial x}(x,T_n)\right|xdx\leq A_9T_n+A_{10}T_n^2+A_{11}T_n^3,$$

then the solution to (**??**) *satisfies*

$$\int_{\mathbb{R}^+}\left|\frac{\partial u}{\partial x}(x,t)\right|xdx\leq A_8e^{A_7(t-T_n)}+A_9t+A_{10}t^2+A_{11}t^3+A_{12}T_ne^{A_7(t-T_n)},\quad t\geq T_n.$$

with

$$A_8=\frac{b_\infty A_6(M_2+M_3)}{A_7},\ A_9=c_\infty(x_M^\xi-x_m^\xi)x_M^\xi\xi_\infty',\ A_{10}=a_\infty\frac{A_3}{2},\ A_{11}=a_\infty\frac{A_2}{3},\ A_{12}=\beta_\infty A_6'.$$

Proof. Let us differentiate equation (**??**) with respect to x and multiply the result by $x\,\mathrm{sign}\left(\frac{\partial u}{\partial x}(x,t)\right)$. This gives

$$\frac{\partial}{\partial t}x\left|\frac{\partial u}{\partial x}\right|(x,t)+a(t)x\frac{\partial}{\partial x}\left|\frac{\partial u}{\partial x}\right|(x,t)=b(t)\Big(-xB(x)\left|\frac{\partial u}{\partial x}(x,t)\right|-x\int_0^x\partial_1k(x,y)dy\,\mathrm{sign}\left(\frac{\partial u}{\partial x}(x,t)\right)u(x,t)$$
$$+\mathrm{sign}\left(\frac{\partial u}{\partial x}(x,t)\right)x\int_x^\infty\partial_2k(y,x)u(y,t)dy\Big)+c(t)\,\mathrm{sign}\left(\frac{\partial u}{\partial x}(x,t)\right)x\frac{\partial\xi}{\partial x}(x).$$

After integration and using the same kind of estimates as those used for Lemma **??**, we have and using Lemma **??**,

$$\frac{d}{dt}\int_{\mathbb{R}^+}x\left|\frac{\partial u}{\partial x}(x,t)\right|dx\le b_\infty A_6(M_2+M_3)e^{A_7t}+a_\infty(A_2t^2+A_3t)+c_\infty(x_M^\xi-x_m^\xi)x_M^\xi\xi'_\infty$$

and the conclusion of Lemma **??** follows after time integration. □

Lemma 7 ($L^1(xdx)$-stability- only for $M_1\neq 0$)**.** *For (a_1,b_1,c_1) and (a_2,b_2,c_2) two triplets of functions of $L^\infty(\mathbb{R}^+)$, the associated solutions u_1 and u_2 to (**??**) satisfy*

$$\int_{\mathbb{R}^+}x|u(x,t)|dx\le A_{13}e^{A_7(t-T_n)}+A_{14}t,\qquad t\ge T_n,$$

where

$$A_{13}=\frac{1}{A_7}+\frac{v}{A_7^2}+\frac{2y}{A_7^3}+\frac{6z}{A_7^4},\qquad A_{14}=(M_1+2B_\infty)\|b_1-b_2\|_\infty A_6,$$
$$v=(A_3\|a_1-a_2\|_\infty+M_0I_\xi c_\infty\|b_1-b_2\|_\infty+M_0I_\xi b_\infty\|c_1-c_2\|_\infty),$$
$$y=M_0((A_2+A_3)\|a_1-a_2\|_\infty+A_5\|b_1-b_2\|_\infty),$$
$$z=M_0A_4\|a_1-a_2\|_\infty.$$

Proof. We multiply the equation (**??**) (satisfied by u) by $x\,\mathrm{sign}(u(x,t))$ and we integrate it over $\mathbb{R}^+$ so that

$$\frac{d}{dt}\int_{\mathbb{R}^+}x|u(x,t)|dx\le -a_1(t)\int_{\mathbb{R}^+}x\frac{\partial|u|}{\partial x}(x,t)dx+|a_1(t)-a_2(t)|\int_{\mathbb{R}^+}x\left|\frac{\partial u_2}{\partial x}(x,t)\right|dx$$
$$+b_1(t)\int_{\mathbb{R}^+}\int_0^x(x-y)k(x,y)|u(x,t)|dx+|c_1(t)-c_2(t)|\int_{\mathbb{R}^+}x\xi(x)dx$$
$$+(b_1(t)-b_2(t))\int_{\mathbb{R}^+}\int_0^xk(x,y)(x\,\mathrm{sign}(u(x,t))-y\,\mathrm{sign}(u(y,t)))u_2(x,t)dx.$$

Then,

$$\frac{d}{dt}\int_{\mathbb{R}^+}x|u(x,t)|dx\le\underbrace{b_\infty M_1}_{A_7}\int_{\mathbb{R}^+}x|u(x,t)|dx+\|c_1-c_2\|_\infty+t^3M_0A_4\|a_1-a_2\|_\infty$$
$$+t^2M_0((A_2+A_3)\|a_1-a_2\|_\infty+A_5\|b_1-b_2\|_\infty)$$
$$+t(A_3\|a_1-a_2\|_\infty+M_0I_\xi c_\infty\|b_1-b_2\|_\infty+M_0I_\xi b_\infty\|c_1-c_2\|_\infty)$$
$$+(M_1+2B_\infty)\|b_1-b_2\|_\infty A_6e^{A_7t},\quad t\in[T_n,T_n+T].$$

A function satisfying $f'(t)\le u+vt+yt^2+zt^3+me^{w(t-T_n)}+m'T_ne^{w(t-T_n)}+wf(t)$ with $f(T_n)=0$ satisfies $f(t)\le\left(\frac{1}{w}+\frac{v}{w^2}+\frac{2y}{w^3}+\frac{6z}{w^4}\right)e^{w(t-T_n)}+mt$, and we obtain Lemma **??**.

□

Lemma 8 (A-priori estimate for the solution)**.** *Let us assume that there exists a solution* $(u,p) \in C(\mathbb{R}^+; L^1(\mathbb{R}^+,(1+x)dx)) \times C(\mathbb{R}^+)$ *to the system* (**??**), (**??**) *with boundary conditions* (**??**) *for* $t \in [0,T_n]$ *for some given* $T_n \geq 0$*. Then, it satisfies*

$$0 \leq p(t) \leq p_0, \qquad \int_{\mathbb{R}^+} u(x,T)xdx \leq p_0, \quad \text{and} \quad \int_{\mathbb{R}^+} u(x,T)dx \leq N(p_0)I_\xi T, \quad \text{for} \quad T \geq 0. \tag{30}$$

$$\text{and} \quad \int_{\mathbb{R}^+} \left|\frac{\partial u}{\partial x}(x,T)\right| dx \leq K_1 T + K_2 T^2, \quad \text{for} \quad T > 0, \tag{31}$$

for some positive constants K_1 *and* K_2 *given by*

$$K_1 = (x_M^\xi - x_m^\xi)N(p_0)\xi'_\infty, \quad K_2 = \frac{\beta(p_0)}{2}N(p_0)I_\xi(M_2+M_3).$$

Proof. The proof of (**??**) is a direct application of Lemma **??**. □

3.4 The map G is a contraction

We now show that **G** is a contractive map.

Lemma 9 (Estimate for $\|p\|_Y$)**.** *We fix* $T_n \geq 0$*. For a couple of functions* $(\bar{p_1},\bar{p_2}) \in Y^2$*, we define* $p_1 = \mathbf{G}[\bar{p_1}]$*,* $p_2 = \mathbf{G}[\bar{p_2}]$*,* $\bar{p}$*: =* $\bar{p}_1$ *-* $\bar{p}_2$ *and* p*: =* p_1 *-* p_2*, where the initial conditions* p_1^**,* p_2^**,* u_1^* *and* u_2^* *are solutions to* (**??**)*,* (**??**)*,* (**??**) *over* $[0,T_n]$*. (We recall that* Y *and* **G** *depend on* T_n*.) Then we have*

1. *In the case* $M_1 = 0$*,*

$$\|p\|_Y \leq T\left(A_{15}(T_n+T)^3 + A_{16}(T_n+T)^2 + A_{17}(T_n+T) + A_{18}\right)\|\bar{p}\|_Y.$$

2. *In the case* $M_1 \neq 0$*,*

$$\|p\|_Y \leq T\left(A_{15}(T_n+T)^3 + A_{16}(T_n+T)^2 + \tilde{A_{17}}(T_n+T) + A_{18} + A_{19}e^{A_7(T_n+T)}\right)\|\bar{p}\|_Y,$$

where

$$\begin{aligned}
&A_{15} = (\beta_\infty M_0 + \gamma_\infty)A_4\alpha, \quad A_{16} = (\beta_\infty M_0 + \gamma_\infty)(A_3\alpha + A_5\beta'_\infty),\\
&A_{17} = N'_\infty I_\xi(\beta_\infty M_0 + \gamma_\infty) + N_\infty I_\xi(\alpha + \beta'_\infty M_0),\\
&\tilde{A_{17}} = A_{17} + M_1\beta_\infty A_{12}, \quad A_{18} = N'_\infty, \quad A_{19} = M_1(\beta'_\infty A_6 + \beta_\infty A_{13}), \quad \tilde{A_{19}} = M_1\beta'_\infty A'_6.
\end{aligned}$$

Proof. We denote by u_i the unique solution of (**??**) with $\bar{p} = \bar{p}_i$. We define $u := u_1 - u_2$. We have

$$\begin{aligned}
\frac{dp}{dt}(t) = &-\gamma(\bar{p_1}(t))\int_{\mathbb{R}^+} u(x,t)dx - (\gamma(\bar{p_1}(t)) - \gamma(\bar{p_2}(t)))\int_{\mathbb{R}^+} u_2(x,t)dx\\
&+ \beta(\bar{p_2}(t))\int_{\mathbb{R}^+} u(y,t)\left(\int_0^y (y-x)k(y,x)dx\right)dy\\
&+ (\beta(\bar{p_1}(t)) - \beta(\bar{p_2}(t)))\int_{\mathbb{R}^+} u_1(y,t)\left(\int_0^y (y-x)k(y,x)dx\right)dy\\
&+ N(\bar{p_1}(t)) - N(\bar{p_2}(t)), \qquad t \in [T_n, T_n+T],
\end{aligned}$$

which after integration over $[T_n, t]$ for $t \in [T_n, T_n + T]$ gives us

$$
\begin{aligned}
|p_1(t) - p_2(t)| \leq & \int_{T_n}^{t} \gamma(\bar{p_1}(s)) \int_{\mathbb{R}^+} |u(x,s)| dx ds + \alpha \int_{T_n}^{t} |\bar{p_1}(s) - \bar{p_2}(s)| \int_{\mathbb{R}^+} u_2(x,s) dx ds \\
& + \beta_\infty \int_{T_n}^{t} \int_{\mathbb{R}^+} |u(y,s)| \left(\int_0^y (y-x) k(y,x) dx \right) dy \\
& + \beta'_\infty \int_{T_n}^{t} |\bar{p_1}(s)) - \bar{p_2}(s)| \int_{\mathbb{R}^+} |u_2(y,s)| \left(\int_0^y (y-x) k(y,x) dx \right) dy ds \\
& + N'_\infty \int_{T_n}^{t} |\bar{p_1}(s) - \bar{p_2}(s)| ds, \qquad t \in [T_n, T_n + T].
\end{aligned}
$$

We take the supremum over $[T_n, T_n + T]$ on both sides such that

$$
\begin{aligned}
\|p\|_Y \leq & T \|\bar{p}\|_Y \left(N'_\infty + \int_{\mathbb{R}^+} (\beta'_\infty (M_0 + M_1 x) + \alpha) \sup_{t \in [T_n, T_n + T]} |u_2(x,t)| \, dx \right) \\
& + T \left(\int_{\mathbb{R}^+} (\gamma_\infty + \beta_\infty (M_0 + M_1 x)) \sup_{t \in [T_n, T_n + T]} |u(x,t)| dx \right).
\end{aligned}
$$

We now use the previous Lemmas that we apply for

$a_\infty = \gamma_\infty,\ b_\infty = \beta_\infty,\ c_\infty = N_\infty,\ \|a_1 - a_2\|_\infty = \alpha \|\bar{p}\|_Y,\ \|b_1 - b_2\|_\infty = \beta'_\infty \|\bar{p}\|_Y,\ \|c_1 - c_2\|_\infty = N'_\infty \|\bar{p}\|_Y.$

We distinguish two cases. First, we consider $M_1 = 0$. Using Lemma (**??**), we have

$$
\int_{\mathbb{R}^+} u_2(x, T_n) dx = \int_{\mathbb{R}^+} u_2^*(x, T_n) dx \leq N(p_0) I_\xi T_n,
$$

so that Lemma (**??**) implies

$$
\int_{\mathbb{R}^+} u_2(x,t) dx \leq N_\infty I_\xi (T_n + T), \qquad t \in [T_n, T_n + T].
$$

Since

$$
\int_{\mathbb{R}^+} \left| \frac{\partial u_2}{\partial x}(x, T_n) \right| dx = \int_{\mathbb{R}^+} \left| \frac{\partial u_2^*}{\partial x}(x, T_n) \right| dx \leq K_1 T_n + K_2 T_n^2 \leq A_2 T_n^2 + A_3 T_n,
$$

we can apply Lemma **??** and obtain

$$
\begin{aligned}
\|p\|_Y \leq & T \|\bar{p}\|_Y \Big(N'_\infty + (T_n + T)(N'_\infty I_\xi (\beta_\infty M_0 + \gamma_\infty) + N_\infty I_\xi (\alpha + \beta'_\infty M_0)) \\
& + (T_n + T)^2 (\beta_\infty M_0 + \gamma_\infty)(A_3 \alpha + A_5 \beta'_\infty) + (T_n + T)^3 (\beta_\infty M_0 + \gamma_\infty) A_4 \alpha \Big)
\end{aligned}
$$

which leads to the conclusion of the first item of Lemma **??**. For the case $M_1 \neq 0$, Lemma **??** implies that

$$
\int_{\mathbb{R}^+} x u(x, T_n) dx \leq p_0
$$

so that we can apply Lemma **??**. We also use Lemma **??** and we obtain

$$
\begin{aligned}
\|p\|_Y \leq & T \|\bar{p}\|_Y \Big(N'_\infty + (T_n + T)(N'_\infty I_\xi (\beta_\infty M_0 + \gamma_\infty) + N_\infty I_\xi (\alpha + \beta'_\infty M_0) + \beta_\infty M_1 A_{14}) \\
& + (T_n + T)^2 (\beta_\infty M_0 + \gamma_\infty)(A_3 \alpha + A_5 \beta'_\infty) + (T_n + T)^3 (\beta_\infty M_0 + \gamma_\infty) A_4 \alpha \\
& + M_1 (\beta'_\infty M_1 (A_6 + A'_6 T_n) + \beta_\infty A_{13}) e^{A_7 T} \Big)
\end{aligned}
$$

which ends the proof of Lemma **??**. □

The next Lemma is the last Lemma required for the proof of Theorem **??**.

Lemma 10. *We can build a sequence $T_0 = 0, T_1, \dots, T_n, T_{n+1}, \dots$ such that*

1. *For all $n \in \mathbb{N}$, there exists a unique solution to system (**??**) (**??**) for $t \in [0, T_n]$,*
2. $\lim_{n\to\infty} T_n = +\infty$.

Proof. Let us assume that (u^*, p^*) is a solution to system (**??**) (**??**) for $t \in [0, T_n]$. For the couple of functions $(\bar{p_1}, \bar{p_2}) \in Y^2$, we define $p_1 = \mathbf{G}[\bar{p_1}]$ and $p_2 = \mathbf{G}[\bar{p_2}]$. Lemma **??** gives us

$$\begin{aligned}\|\mathbf{G}[\bar{p_1}] - \mathbf{G}[\bar{p_2}]\|_Y \leq T\Big(&A_{15}(T_n+T)^3 + A_{16}(T_n+T)^2 + \tilde{A_{17}}(T_n+T) + A_{18} + A_{19}e^{A_7T} \\ &+ \tilde{A}_{19}T_ne^{A_7T}\Big)\|\bar{p_1} - \bar{p_2}\|_Y,\end{aligned} \tag{32}$$

where the $A_i's$ are those defined in Lemma **??**. The map $\mathbf{G}$ is a strict contraction provided that the sum in (**??**) is strictly less than 1, which is implied by the fact that each of the 6 terms is strictly less than 1/6. As a consequence, the map $\mathbf{G}$ is a strict contraction over $[T_n, T_n + T]$ as soon as T satisfies the 5 following conditions:

$$T < \frac{1}{6A_{18}} =: G_1(T_n),\ T < \frac{1}{6\tilde{A}_{17}\left(T_n + \frac{1}{6A_{18}}\right)} =: G_2(T_n),\ T < \frac{1}{6A_{16}\left(T_n + \frac{1}{6A_{18}}\right)^2} =: G_3(T_n),$$

$$T < \frac{1}{6A_{15}\left(T_n + \frac{1}{6A_{18}}\right)^3} =: G_4(T_n),\ T < \frac{1}{A_{19}}e^{-A_7\left(T_n + \frac{1}{6A_{18}}\right)} =: G_5(T_n),$$

$$T < \frac{1}{A_{19}T_n}e^{-A_7\left(T_n + \frac{1}{6A_{18}}\right)} =: G_6(T_n).$$

Then, the Banach fixed point theorem guarantees that we can extend the solution to $[T_n, T_n + T]$. The sequence defined by induction through

$$T_0 = 0, \qquad T_{n+1} = T_n + \min\{G_1(T_n), G_2(T_n), G_3(T_n), G_4(T_n), G_5(T_n), G_6(T_n)\},$$

is diverging, since it is strictly increasing and the application $x \to x + \min\{G_1(x) + G_2(x) + G_3(x) + G_4(x) + G_5(x) + G_6(x)\}$ has no fixed point.

□

4 Numerical results

In this section, we describe results of the numerical simulation of equations (**??**), (**??**), and (**??**). First, we outline the numerical details of our approach. Then, we illustrate the behavior of our model by running a variety of simulations. In particular, we show how variations in certain model parameters change the qualitative and quantitative behavior of solutions. Such exploration gives us a better idea as to which parameters might be influenced by the addition of MTAs into a system of growing MTs. We focus our study on the action of vinblastine, a member of the destabilizing vinca alkaloid family. We do this since there are a number of studies which indicate how this drug might

alter certain dynamics properties of MTs which we account for in our modeling framework [**?**, **?**, **?**]. We simulate our model using a finite difference method. For the advection terms in equation (**??**) we use an upwinding approach, and an explicit Euler strategy for the ODEs (**??**) and (**??**). All integral terms are calculated using an order 0 quadrature method, adjusted to preserve tubulin at the discrete level.

We discretize our domain into 100 grid points, where the distance between each grid point, Δx, is constant and equal to 0.2μm. Our domain is between 10 μm and 100μm in length, depending on the parameters, insuring that the support of $u(., t)$ stays in the numerical domain for all time.. Also, we choose an appropriate time step so that our scheme satisfies the CFL condition [**?**]. Our time step, Δt, equals 0.001 seconds.

4.1 Parameter values in the base case

Our base-case parameters for the numerical simulations are summarized in Table **??**. For some model parameters, their order of magnitude was determined from the literature. In particular, the growth parameter α and the GDP/GTP-tubulin exchange rate κ fall within the ranges of those given in [**?**], the hydrolysis rate is found in [**?**], the shortening rate β_∞ in [**?**], and the dimer nucleation number m in [**?**, **?**]. Other parameters were estimated in this paper, or selected through experimental observations of Honoré (experimental results not shown here, but experimental conditions are the same as those of [**?**]). All model parameters, along with how they were selected, are summarized in Table **??**.

4.2 Simulation results in the base case

We first describe simulation output that can be compared with experimental data.

One quantity of interest is the mean concentration of tubulin in polymerized form. This average, between T_{min} and T_{max}, is defined as

$$\bar{M} = \frac{1}{T_{max} - T_{min}} \int_{T_{min}}^{T_{max}} M(t)dt, \tag{33}$$

where tubulin in polymerized form at time t is defined as,

$$M(t) = \int_0^\infty u(x,t)xdx.$$

The value T_{min} is the time at which the first GTP-tubulin population begins to stabilize (we will describe this in more detail later in this section), T_{max} is the maximum time of simulation.

Similarly, we can write the mean MT growth rate as

$$\bar{\gamma} = \frac{1}{T_{max} - T_{min}} \int_{T_{min}}^{T_{max}} \gamma\left(p(t)\right) dt. \tag{34}$$

This quantity allows the calibration of the growth parameter α in formula (**??**). The mean growth speed has been determined experimentally as 4.7 ± 1.4 $\frac{\mu\text{m}}{\text{min}}$ using data collected from kymographs (recall Figure **??**). This is within the range recorded in [**?**] (and close to that found in [**?**]). The output of the model gives us a mean growth rate of $\bar{\gamma} = 5.2\frac{\mu\text{m}}{\text{min}}$.
Figures **??** (Left) and (Right) illustrate oscillating populations of tubulin in polymer form as well as oscillating populations of free GTP- and GDP-tubulin using the base-case model parameters given in Table **??**.

Table 1: **Table of model parameters**

Model parameter	**Description**	**Value**	**Source**
α	Growth parameter	$2\ \frac{\mu\text{m}}{\mu\text{M}\cdot\text{min}}$	Within range found in [**?**, **?**]
γ^h	Baseline hydrolysis rate	$5\ \frac{\mu\text{m}}{\text{min}}$	Similar to that in [**?**]
β_∞	Shortening rate	$20\pm7.8\ \frac{\mu\text{m}}{\text{min}}$	Within range found in [**?**]
x_0	Shortening distance	$1.6\pm\ 1.2\ \mu$m	[This paper]
σ	Standard deviation of x_0	$0.2\ \mu$m	[This paper]
μ	Nucleation rate	$0.1\ \frac{1}{\text{M}\cdot\text{min}}$	[This paper]
m	Dimer nucleation number	2	[**?**, **?**]
C_N	Normalization constant (from equation (**??**)) C_N	1/4	[Estimated using equation (**??**)]
x_{min}	Maximal size of nucleated MTs	$0.8\ \mu$m	[This paper]
κ	GDP/GTP-tubulin exchange rate	$2\ \frac{1}{\text{min}}$	Within range found in [**?**]
p_c	Critical growth value	$2\ \mu$M	[This paper - Typically can be higher, $\approx 5\ \mu$M [**?**]]
p_N	Critical nucleation value	$12\ \mu$M	[This paper]
p_0	Initial GTP concentration	$15\ \mu$M	Within standard GTP concentration range [**?**]
p_h	Critical fragmentation value	$4.5\ \mu$M	[Estimated using equation (**??**)]

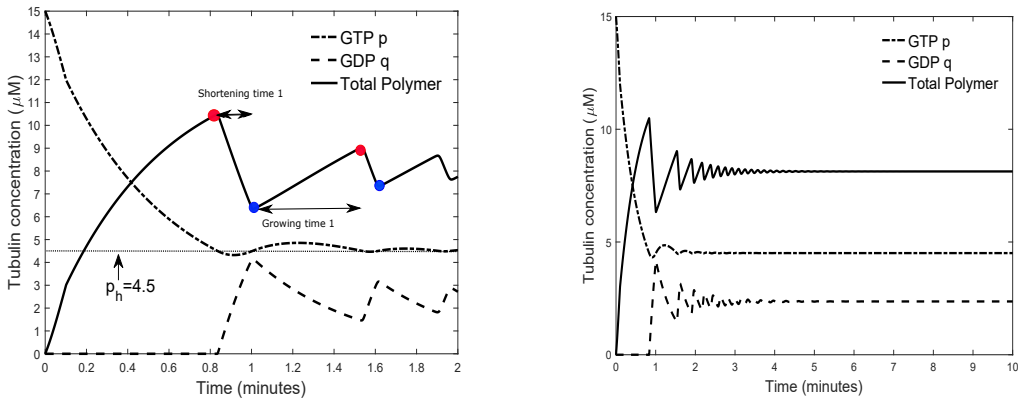

Figure 4: Left: Example of oscillating populations of tubulin found in MTs, free GTP-tubulin, and free GDP-tubulin. Parameters used are summarized in Table **??**. Shortening kernel k_0 is used. Right: Extended simulation of the figure to the left. MT dynamic instability is only sustained over a relatively short period of time. For large time, MT dynamics are completely suppressed.

In Figure **??** (Left), we show the time evolution of the three tubulin populations (GTP tubulin, GDP tubulin, and tubulin in polymerized form) and we highlight population-level catastrophe and rescue events by red dots and blue dots, respectively. Also, examples of shortening and growing time periods are highlighted. Figure **??** (Right) shows the long-time simulation (steady-state solutions) of that described on the left.

Using Figure **??** (Left), we calculate values for the mean MT length $\bar{u}_{tot}$ and growth rate $\bar{\gamma}$, using formulas (**??**) and (**??**), where T_{min} is set to T_1 (the time of the first catastrophe event). These values are given by 7.9μM and $5.2\frac{\mu\text{m}}{\text{min}}$, repectively. From Figure **??** (Left), we see that at T_1 the GTP-tubulin concentration approaches a mean value which is close in value to p_h (4.5μM, see Table **??**).

The value of p drives the system through the nucleation rate $N(p)$, the shortening rate $\beta(p)$, and the growth rate $\gamma(p)$. Recall that, the critical nucleation value $p_N = 12\mu$M, the critical growth value $p_c = 2\mu$M and the critical fragmentation value $p_h = \dfrac{\gamma^h + \alpha p_c}{\alpha} = 4.5\mu$M. At time $t = 0$, $p = 15\mu$M, thus $N(p) > 0$, $\beta(p) = 0$ and $\gamma(p) > 0$: new microtubules are formed by nucleation and they grow so that the total mass of microtubules increases and p decreases. From Figure **??** (Left), at time $t = 0.1$, p goes below the critical nucleation value p_N; from that point, nucleation stops, which slows down the creation of polymerized tubulin. At time $t = 0.8$, p reaches the critical value p_h and fragmentation is initiated: microtubules start to shorten, and free GDP-tubulin (q) is created. We notice that the amplitude of the oscillations, as well as the period of oscillation, decrease with time. This result suggests that MT oscillations may be sustained over a relatively short period of time. However, at the individual level the MT instability is still present.

4.3 Influence of β_∞ and x_* for the two kernels

In this section, we show simulation results for system (**??**), (**??**), and (**??**) for the different shortening kernels, k_0 and k_1, described in equation (**??**). First, we observe that for the range of parameters tested, both macroscopic variables (U, p, q), where $U(t) = \int_{\mathbb{R}} u(x,t)dx$ and the microtubules size distribution $u(x,t)$ converge to some steady state in large time. On both Figure **??** and Figure **??** are displayed the time-evolution of the macroscopic variables (U, p, q) (bottom) and the final profile of the microscopic variable u (up) for kernels k_0 (left) and k_1 (right). We consider that

microscopic equilibrium is reached numerically as soon as for some t, we have the criterion $\|u(.,t) - u(.,t+dt)\|_\infty \leq 10^{-10}$ satisfied. Notice that macroscopic equilibrium is reached before microscopic equilibrium. On Figure **??**, we explore the dependence on x_*. In the range of biologically relevant parameters ($x_0 \leq 5$ and $x_1 \leq 5$), the macroscopic behaviour does not quantitatively depend on x_*: p converges to p_h, and q and U converge to some value inedpendent of x_*. The transient behaviour is qualitatively the same as well: the relaxation toward steady state occurs after a few oscillations. The only difference lies in the transient behaviour, on the time at which equilibrium is reached (that strongly depends on x_*, for $x_0 = 5$, $T_\infty \approx 60$ and for $x_0 = 1.6$, $T_\infty \approx 180$ for instance) and on the shape of the stationary profile for u. For larger values of x_* however (here $x_1 \geq 10$ and $x_0 \geq 20$ (results not shown for x_0)), it may happen that p converges in large time to a value smaller than p_h, and close to p_c. On Figure **??**, we explore the dependence on β_∞. Here again, for biologically relevant values for β_∞ ($\beta_\infty \geq 5$ for k_0, $\beta_\infty \geq 1$ for k_1), the steady state does not depend on β_∞: after damped oscillations, p converges to p_h and and q and u also converge to some values and profile independent on β_∞. However, for smaller values of β_∞, p converges to some $p(\beta_\infty) \neq p_h$, and so do q and u. In Section **??**, we give an insight on how these behaviours can be intuited directly from a mathematical analysis of the system.

4.4 Dependence of p_h on MT dynamics: insight into drug effects

In this section, we show how variations in p_h change the total polymerized tubulin and GTP-tubulin concentration. We do so in order to test whether our results are consistent with what we know about how changes in this parameter (due to variations in MTA concentration) alter MT dynamics. In *in vitro* experiments it has been shown that high concentrations of vinblastine [**?**, **?**], a member of the vinca alkaloid family, promotes MT depolymerization. However, at low doses of this drug, it suppresses MT dynamic instability. Specifically, MT growth rates and shortening rates decrease, while catastrophe is suppressed. Further, shortening lengths are also decreased. These dynamic changes result in almost constant overall polymer mass (with only minor MT depolymerization). However, in the presence of EBs, which is the case in cells, vinblastine increases catastrophe frequency, slightly increases the MT growth rate, and decreases MT growth length [**?**].
Figure **??** corresponds to simulation results for changes in the critical fragmentation value p_h (i.e., the hydrolysis rate) from the base-case value (see Table **??**). From Figure **??**(left), we see a decrease in tubulin in polymer form u_{tot} for increasing p_h. Further, we see that increases in p_h (from the base case) work to promote MT dynamics by increasing the number of catastrophe events. Figure **??**(right) shows the corresponding changes in the GTP-tubulin concentration. Here, it is noted that as p_h increases, which corresponds to an increase in the hydrolysis rate γ^h, the level of free GTP-tubulin in the system increases. This result makes sense, due to the fact that as a MT depolymerizes (at high values of the hydrolysis rate), free tubulin is released back into the system.

Vinblastine binds to free tubulin rapidly (and reversibly) and also binds to the extreme end of MTs [**?**]. At high concentrations, vinblastine has also been shown to bind (with low affinity) to sites along the MT surface, which is believed to help induce the peeling of protofiliments at the MT ends. These drugs bind to the vinca domain near the GTP hydrolyzable site on β - tubulin, and act on MTs (at higher concentrations) by the reducing the GTP-cap size [**?**], while having little effect on the MT growth rate (this remains near constant). This phenomenon is linked to the speeding up of GTP hydrolysis, which corresponds to an increase in p_h in our model. This mechanism of action is not only seen at high depolymerizing concentrations, but also at low concentrations in the presence of EBs [**?**]. Our results are consistent with these observations. In particular, increasing GTP hydrolysis aids in MT depolymerization (shown in Figure **??**).

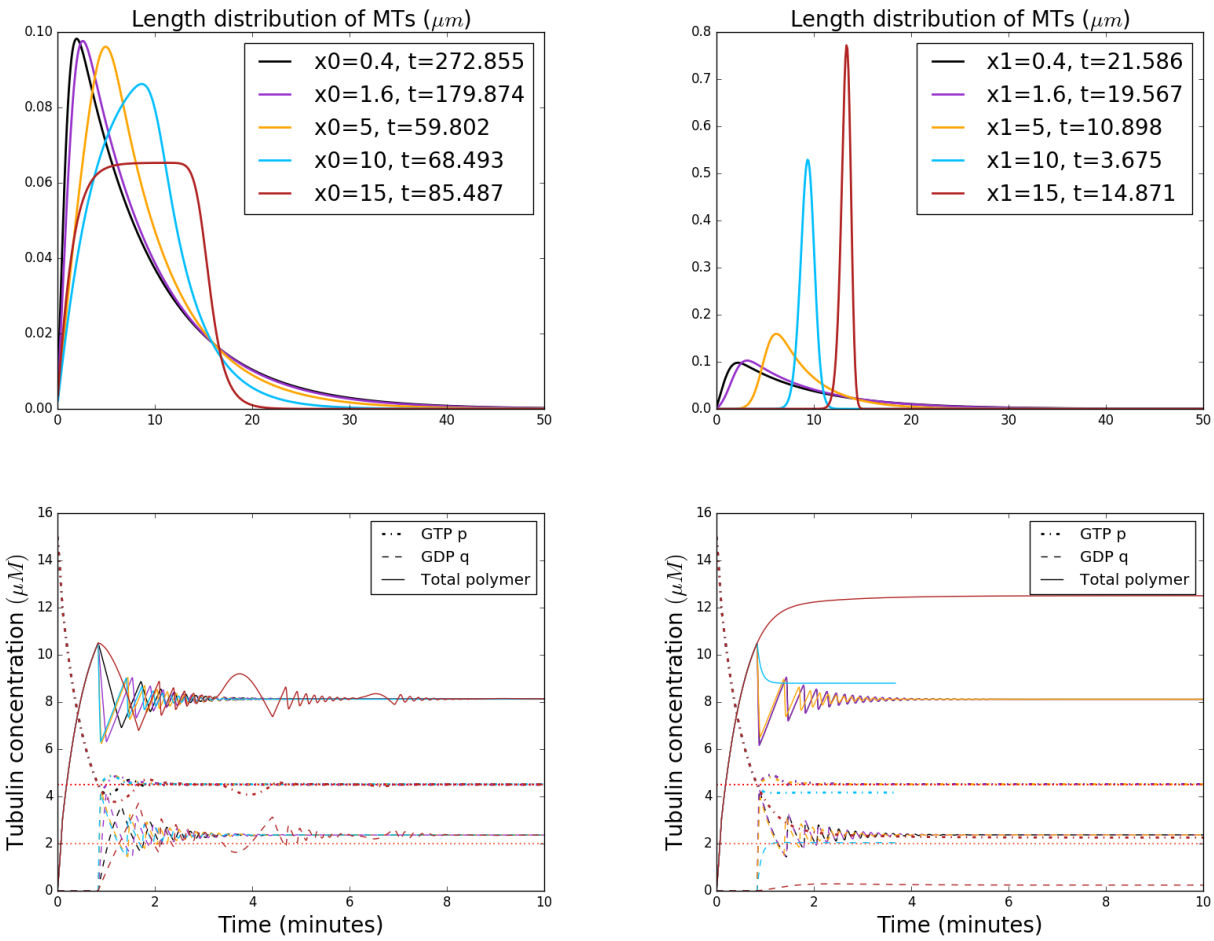

Figure 5: Comparison of the different transient behaviours for the macroscopic variables (U, p, q) (bottom) and asymptotic behaviour for the variable u for different values of x_0 and x_1. Left: k_0, Right: k_1.

4.5 Asymptotic profile for u with respect to initial condition

In this paragraph, we consider a fragmentation kernel of type k_0 (equation (**??**)) with $\sigma = 1$ and all the parameters given in Table **??** except for $p_h = 6$ and the initial condition. All the plots displayed on Figure **??** are obtained for $p_0 = 11$, $q_0 = 0$, and four different initial size distributions IC1: $u_0(x) = u_{5,10}(x)$, IC2: $u_0(x) = u_{5,10}(x) + u_{10,10}(x)$, IC3: $u_0(x) = u_{10,1}(x)$, IC4: $u_0(x) = u_{5,1}(x)$, where

$$u_{x_c,\sigma}(x) = \exp\left(-\frac{(x - x_c)^2}{\sigma}\right),$$

and all the initial profiles being rescaled to satisfy $\int_{\mathbb{R}^+} x u_0(x) dx = 1$. The numerical results suggest that the system relaxes toward an equilibrium state, i.e. that p and q converges toward some limiting values p^* and q^*, and that the size distribution $u(x, t)$ converges toward an asymptotic profile $u^*(x)$. The limiting value for p is $p^* = p_h$ and the value for q^* (see Figure **??**, upper left) and then the asymptotic profile u^* both depend on the initial distribution u_0 (see Figure **??**, upper right and Figure **??**). The initial value p_0 is small enough so that there is no nucleation at time $t = 0$, and the numerical simulations show that the value of $p(t)$ always stay below the threshold

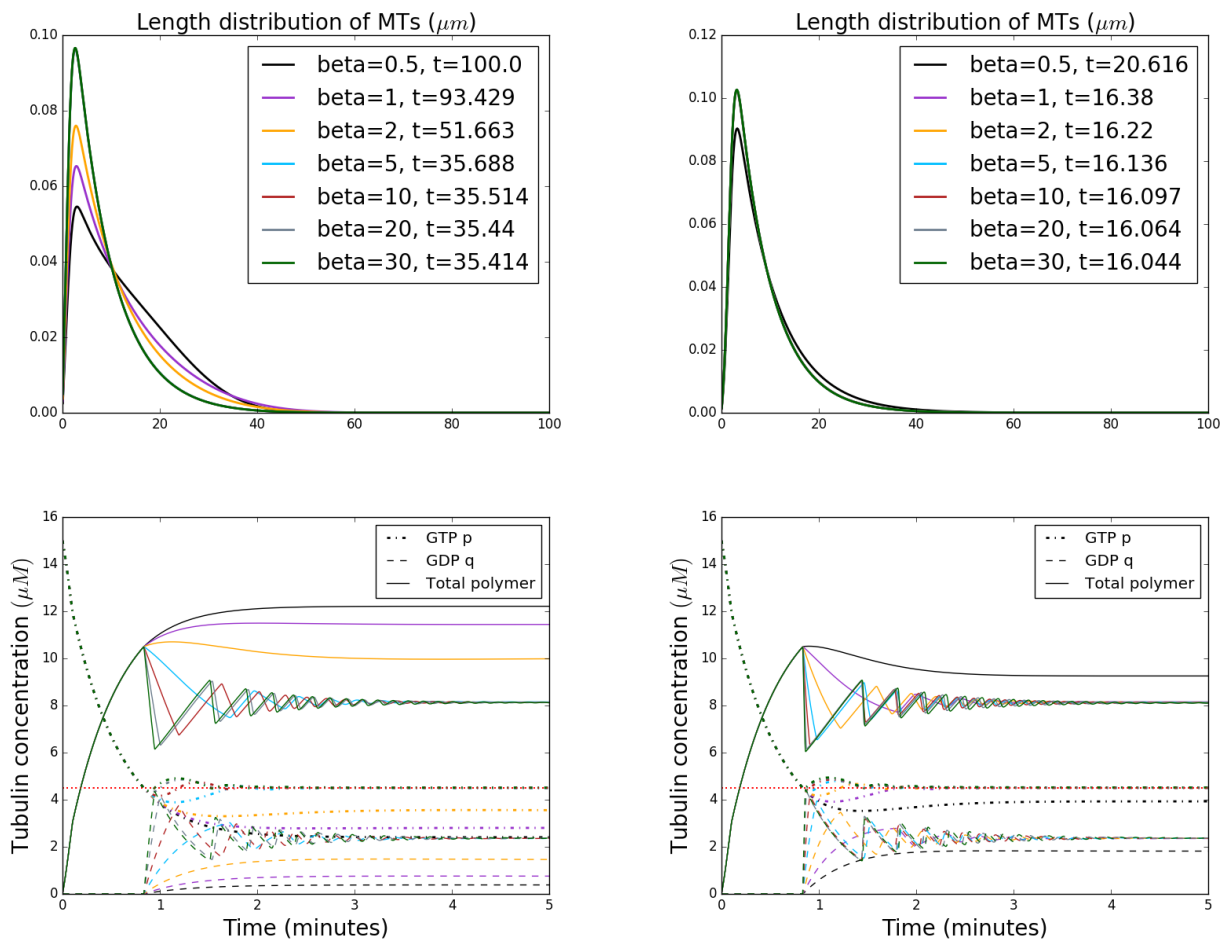

Figure 6: Comparison of the different transient behaviours for the macroscopic variables (U, p, q) (bottom) and asymptotic behaviour for the variable u for different values of β_∞. Left: k_0, Right: k_1.

that triggers nucleation. As a consequence, the total number of polymers $\int_{\mathbb{R}^+} u(x,t)dx$ is preserved over time. The initial number of polymers is closed for IC1 and IC4 (respectively 0.197 and 0.2), and stay close for all time. Since at the beginning of the dynamic, fragmentation is turned off (i.e. $p(t) \geq p_h$, see Figure **??**, upper left) the evolution of the system (u, p, q) only depends on $p(t)$, $q(t)$ and $\int_{\mathbb{R}^+} u(x,t)dx$ (see system (**??**)(**??**)(**??**)) which explains why the time evolution of the macroscopic quantities for IC1 and IC4 are almost superimposed (Figure **??**, upper left).

Our guess is that the asymptotic state satisfies

$$\gamma(p_h)\frac{\partial u^*}{\partial x}(x) = \beta(p_h)\left(-\int_0^x k(x,y)dy\; u^*(x) + \int_x^\infty k(y,x)u^*(y)dy\right) + N(p_h)\xi(x), \tag{35}$$

and $q^* = \dfrac{\gamma(p_h)}{\kappa}\displaystyle\int_0^{+\infty} u^*(x)dx + \dfrac{N(p_h)}{\kappa}$.

Proving that the steady state (u^*, p_h, q^*) is attractive is a difficult problem. Long-time asymptotic behaviour for general growth fragmentation equations has been described in [**?**] using semi-group theory. For systems of equations, the problem is more tricky. Some work in this direction has been initiated in [**?**], but no proof of convergence has been shown. In the general case, due to the

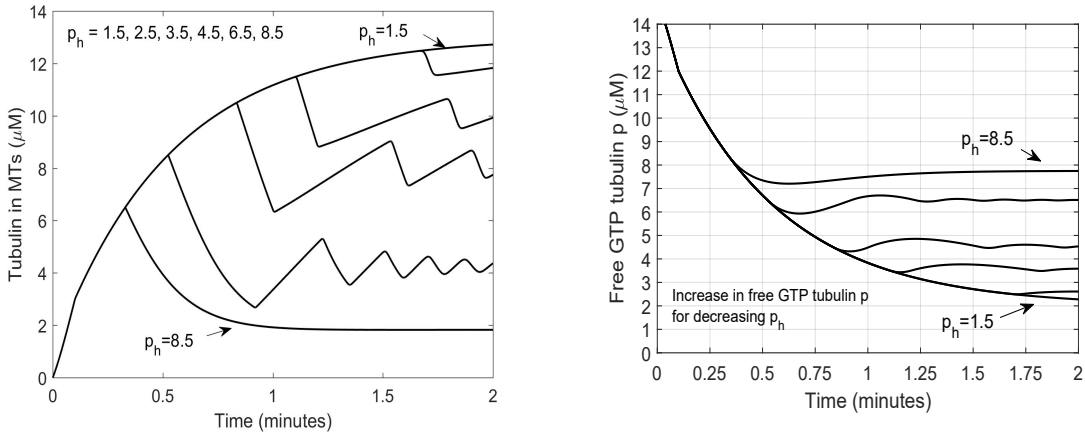

Figure 7: Left: Changes in polymerized tubulin due to variations in the hydrolysis rate. Right: Variation of the free GDP-tubulin $p(t)$ with respect to p_h.

structure of kernels k_0 and k_1, the system can not be reduced to a close ODE system in (U, p, q) as it was done for similar systems [**?**]. However, it can be for very specific kernels, and this enables us to give an insight on the qualitative asymptotic behaviour we expect for the general system.

4.6 Asymptotic behaviour on a simplified model.

A study can be performed on very simplified model, in the case of a simplified island kernel $k_1(y, x) = \delta_{x_1}(x)$ for $x_1 \geq 0$.

$$\begin{cases} \dfrac{\partial u}{\partial t} + \gamma(p(t))\dfrac{\partial u}{\partial x} = \beta_\varepsilon(p(t))\left(-u(x,t)\chi_{x\geq x_1} + \delta_{x=x_1}\displaystyle\int_{x_1}^{\infty} u(y,t)dy\right) + \mu H_\varepsilon(p(t), p_N)p(t)^2\xi(x), \\ p'(t) = -\gamma(p(t))\displaystyle\int_0^\infty u(x,t)dx + \kappa q(t) - \mu H_\varepsilon(p(t), p_N)p(t)^2, \\ q'(t) = -\kappa q(t) + \beta_\varepsilon(p(t))\displaystyle\int_0^\infty (x - x_1)u(x,t)dx, \\ \qquad u(x,0) = u_0(x), \quad u(0,t) = 0, \quad p(0) = p_0, \quad q(0) = 0. \end{cases} \tag{36}$$

This type of kernel does not satisfy the technical assumptions (**??**) guaranteing well-posedness of the model, since it is not a smooth function, but can be seen as a limit case of gaussian kernels k_1^δ centered in x_1. If we integrate the first line of (**??**) we obtain the closed system

$$\begin{cases} U'(t) = \mu H_\varepsilon(p(t), p_N)p(t)^2 I_\xi, \\ p'(t) = -\gamma(p(t))U(t) + \kappa q(t) - \mu H_\varepsilon(p(t), p_N)p(t)^2, \\ q'(t) = -\kappa q(t) + \beta_\varepsilon(p(t))\left(M_0 + p_0 - p(t) - q(t) - x_1 U(t)\right), \\ \qquad U(0) = U_0 \geq 0, \quad p(0) = p_0 \geq 0, \quad q(0) = 0. \end{cases} \tag{37}$$

where $U(t) = \displaystyle\int_0^\infty u(x,t)dx$, $U_0 = U(0)$ and $M_0 = M(0)$. We assume

$$H_\varepsilon(p,z) = \begin{cases} 0 & p \leq z - \varepsilon, \\ 1 & p \geq z + \varepsilon, \end{cases} \quad \frac{\partial}{\partial p}H_\varepsilon(p,z) > 0, \quad \beta_\varepsilon(p) = \beta_\infty\left(1 - H_\varepsilon(p, p_h)\right), \quad H_\varepsilon \in Lip(\mathbb{R}\times\mathbb{R}), \tag{38}$$

and the technical hypotheses

$$x_1 I_\xi < 1, \quad M_0 - x_1 U_0 \geq 0, \tag{39}$$

and

$$\gamma \text{ satisfies } (\mathbf{??}), \quad \gamma \in \mathcal{C}^\infty(\mathbb{R}^+). \tag{40}$$

Proposition 1 (Existence and uniqueness of global solutions for (**??**))**.** *Assuminig* (**??**)*,* (**??**)*, and* (**??**)*, there exists a unique global solution to* (**??**)*.*

Proof. Local existence and uniqueness are guaranteed by the Cauchy Lipschitz theorem. We now prove that the maximal solution defined on $[0, T)$ for some $T > 0$ is positive and uniformly bounded with time. Since $U_0 \geq 0$, first line of (**??**) implies that $U(t) \geq 0$ for $t \in [0, T)$. We denote

$$w(t) = M_0 + p_0 - p(t) - q(t) - x_1 U(t). \tag{41}$$

System (**??**) and assumption $x_1 I\xi < 1$ implies

$$\begin{aligned} w'(t) &= -p'(t) - q'(t) - x_1 U'(t) \\ &= \gamma(p(t))U(t) + \mu H_\varepsilon(p(t), p_N)p^2(t)\,(1 - x_1 I_\xi) - \beta_\varepsilon(p(t))w(t) \geq -\beta_\varepsilon(p(t))w(t), \end{aligned} \tag{42}$$

which gives $w(t) \geq 0$ since assumption (**??**) implies $w(0) \geq 0$. Assume now by contradiction that there exists some $t_1 \leq T$ such that $q(t_1) < 0$. Then, since $q(0) \geq 0$, there exists $0 \leq t_0 < t_1$ such that $q(t_0) = 0$ and $q(t) \leq 0$ for $t \in [t_0, t_1]$. Then, using the mean value theorem, there is $\bar{t} \in [t_0, t_1]$ such that $q'(\bar{t}) < 0$, whereas using third line of system (**??**) and the non negativity of w, we have $q'(\bar{t}) = -\kappa q(\bar{t}) + \beta(p(\bar{t}))w(\bar{t}) \geq 0$, which is absurd. As a consequence, for all $t \in [0, T]$, $q(t) \geq 0$. We do the same for p, assuming again by contradiction that there exists some $t_1 \leq T$ such that $p(t_1) < 0$. Using the same argument than for q, there exists $0 \leq t_0 < t_1$ such that $p(t_0) = 0$ and $p(t) \leq 0$ for $t \in [t_0, t_1]$ and $\bar{t} \in [t_0, t_1]$ such that $p'(\bar{t}) < 0$, whereas using second line of system (**??**), we have $p'(\bar{t}) = -\gamma(p(\bar{t}))U(\bar{t}) + \kappa q(\bar{t}) - \mu H_\varepsilon(p(\bar{t}), p_N)p(\bar{t})^2 \geq 0$, using here that $q(\bar{t})$ is non negative. As a consequence, for all $t \in [0, T]$, $p(t) \geq 0$. In conclusion, the solution is non negative and uniformly bounded, and then the maximal solution is global. □

For the next result, we assume for simplicity that nucleation is turned off, i.e. $\mu = 0$. This enables to guarantee that the quantity U does not evolve with time. System (**??**) then becomes

$$\begin{cases} p'(t) = -\gamma(p(t))U_0 + \kappa q(t), \\ q'(t) = -\kappa q(t) + \beta_\varepsilon(p(t))\,(M_0 + p_0 - p(t) - q(t) - x_1 U_0)\,, \\ \qquad p(0) = p_0 \geq 0, \quad q(0) = 0. \end{cases} \tag{43}$$

The following proposition expresses that for ε small enough, for x_1 larger than a threshold value $\bar{x}$, then the limiting value for p is very close to p_h, and for for x_1 smaller than the threshold value $\bar{x}$, we have the limiting value for p is very close p_h for β_∞ larger than a threshold value $\bar{\beta}$, but for $\beta_\infty < \bar{\beta}$ it may happen that the limiting value for p is smaller than p_h. This is in accordance with what is observed numerically for the complete system.

Proposition 2. *Assuming* (**??**)*, then the system* (**??**) *has a unique equilibrium point* $(p^*_\varepsilon, q^*_\varepsilon)$ *on* $\mathbb{R}^+ \times \mathbb{R}^+$*, this point is asymptotically stable and satisfies*

- *if* $\beta_\infty < \bar{\beta}(x_1)$*, then* $p^*_\varepsilon \in [0, p_h - \varepsilon)$*,*

- *if* $\beta_\infty \geq \bar{\beta}(x_1)$*, then* $p^*_\varepsilon \in [p_h - \varepsilon, p_h + \varepsilon]$*,*

with

$$\bar{x} = \frac{M_0 + p_0 - (p_h + \varepsilon)}{U_0} - \frac{\gamma(p_h + \varepsilon)}{\kappa}, \quad \bar{\beta}(x_1) = \frac{\gamma(p_h - \varepsilon)}{\bar{x} - x_1 + \dfrac{2\varepsilon}{U_0} + \dfrac{\gamma(p_h + \varepsilon) - \gamma(p_h - \varepsilon)}{\kappa}}.$$

Proof. **Equilibrium.** The equilibrium points (p^*, q^*) (we omit the index ε to lighten the notations) are solutions to

$$\gamma(p^*)U_0 = \kappa q^*, \quad \kappa q^* = \beta_\varepsilon(p^*)\left(M_0 + p_0 - p^* - q^* - x_1 U_0\right). \tag{44}$$

Then

$$q^* = \frac{\gamma(p^*)U_0}{\kappa} \tag{45}$$

and p^* necessarily satisfies $\Phi(p^*) = 0$, with

$$\Phi(p) = \beta(p)W(p) - \gamma(p)U_0, \quad W(p) = M_0 + p_0 - p - \frac{U_0\gamma(p)}{\kappa} - x_1 U_0.$$

We first notice that $\Phi(p_h + \varepsilon) = -\gamma(p_h + \varepsilon)U_0 < 0$ and that for $p \geq p_h + \varepsilon$, $\Phi'(p) = -\gamma'(p)U_0 \leq 0$, then the solutions to $\Phi(p) = 0$ belong to $[0, p_h + \varepsilon)$. Also notice that $\Phi(0) = W(0) > 0$, so that Φ has at least one zero $[0, p_h + \varepsilon)$. We also notice that $W'(p) < 0$ for $p \geq 0$. We now distinguish different cases.
Case 1. $W(p_h + \varepsilon) > 0$ *which is* $x_1 < \bar{x}$*.* In that case, for $p \in [0, p_h + \varepsilon)$, $W(p) > 0$ and then $\Phi'(p) < 0$. Then, there exists one unique $p \in [0, p_h + \varepsilon)$ such that $\Phi(p^*) = 0$.
Case 2. $W(p_h + \varepsilon) \leq 0$ *which is* $x_1 \geq \bar{x}$*.* Then, there exists a unique $\bar{p} \in [0, p_h + \varepsilon]$ such that $W(\bar{p}) = 0$, and then $\Phi(\bar{p}) < 0$. As a consequence, there exits $p^* \in [0, \bar{p}]$ such that $\Phi(p^*) = 0$. For $p \in [0, \bar{p}]$, we have $W(p) > 0$, thus $\Phi'(p) < 0$ which guarantees that there is no other solution of $\Phi(p) = 0$ for $p \in [0, \bar{p}]$, and for $p \in [\bar{p}, p_h + \varepsilon]$, we have $\Phi(p) < 0$, which guarantees that there is no other solution of $\Phi(p) = 0$ for $p \in [\bar{p}, p_h + \varepsilon]$. In both cases 1 and 2, depending on the sign of $\Phi(p_h - \varepsilon)$, we give finer estimates on p^*.
Sub-case a. $\Phi(p_h - \varepsilon) < 0$ **which is** $\beta_\infty < \bar{\beta}(x_1)$**.** Here, the unique solution p^* lies in $[0, p_h - \varepsilon)$.
Sub-case b. $\Phi(p_h - \varepsilon) \geq 0$ **which is** $\beta_\infty \geq \bar{\beta}(x_1)$**.** Now, the the unique solution p^* lies in $[p_h - \varepsilon, p_h + \varepsilon]$.
Stability. In all the cases, the study of the Jacobian matrix of the system at (p^*, q^*) gives the asymptotic stability of the unique equilibrium point. Indeed, the jacobian matrix is given by

$$A(p^*) = \begin{pmatrix} -U_0\gamma'(p^*) & \kappa \\ \beta'(p^*)w(p) + \beta(p)w'(p) & -\kappa - \beta(p^*) \end{pmatrix} \tag{46}$$

so that for $p^* \in [0, p_h + \varepsilon)$,

$$\begin{aligned} Tr(A) &= -\kappa - \beta(p^*) - U_0\gamma'(p^*) < 0, \\ Det(A) &= U_0\gamma'(p^*)(\kappa + \beta(p^*)) - \kappa\beta'(p^*)w(p^*) - \kappa\beta(p^*)w'(p^*) > 0, \end{aligned} \tag{47}$$

using $w'(p^*) < 0$ and $\beta(p^*) > 0$. □

5 Conclusions and perspectives

In this paper, we have developed a novel integro-PDE modeling approach to describe MT dynamic instability. Using parameter values calibrated from experiment or taken from the literature, we are able to simulate MT dynamics that are consistent with experiment. Further, through parameter variation, we are able to describe possible mechanisms for how destabilizing MTAs, like vinblastine, work to alter MT dynamics. In the future, it would be interesting to investigate alternate mechanisms for how MTAs alter MT dynamics, as well as how stabilizing drugs can work to alter MT dynamics. Unlike the destabilizing vinca alkaloids, stabilizing drugs like those from the taxane family bind poorly to free tubulin. Instead, they bind with high affinity to tubulin along the length of a MT [**?**, **?**], increasing the rescue frequency by stabilizing the MT lattice. At moderate to high doses, these drugs promote MT polymerization, resulting in a reduced numbers of catastrophe events and high polymerized tubulin concentrations [**?**, **?**].

In addition to understanding how MTAs alter normal MT dynamics, it would be useful to consider ways to extend our model in such a way as to produce stable limit cycles (or oscillations that persist for longer periods of time). This is one of the limitations of our model, as we currently are only able to sustain oscillations for short time periods. However, as this is a population-level model, this does not mean that oscillations do not exist at the microscopic level. One reason for why our model behaves in this way (does not sustain oscillations) is that we assume MT shortening events occur at the time when the hydrolysis rate and the growth rate are equal, thus we are simplifying what is happening in real systems. In particular, in real systems MTs grow through the addition of GTP tubulin. Once GTP tubulin is incorporated into the MT, it is hydrolyzed to lower energy GDP-tubulin, creating a distinct GTP region at the front of a MT (the GTP cap region). When the hydrolysis rate is larger than the growth rate, the MT cap (which we do not account for in this model) shortens. Once it disappears, then a shortening event occurs. In future work, we could account for this by incorporating a time delay at the moment in time when the hydrolysis rate becomes greater than the MT growth rate. However, this would greatly increase the complexity of our model analysis, and is beyond the scope of this paper. The understanding of relaxation toward equilibrium of such systems is also a topic of interest and a future mathematical study will be carried out in that direction.

6 Appendix

About the advantages of our modeling approach over existing ones. We ran a comparative simulation of both models (parameters used are highlighted in figure captions). On Figure **??** we observe that the long-term (averaged) concentrations are very similar. For the full model, we look at the average concentrations from T=3 to 8 minutes. For the new model here, we took the steady-state values (all model parameters used in this model are the same as those for the full model in [31], where the full model also has a few extra parameters - these values are recorded in the figure caption). Mean tubulin concentrations (uM) for full model (previous ref [25], now [31]):
Total polymer: 9.73, GTP - p: 4.35, GDP - q: 0.9095. Mean tubulin concentrations (uM) for this model: Total polymer: 8.13, GTP - p: 4.095, GDP - q: 2.36. These results indicate that our new model does well at qualitatively replicating results in terms of tubulin concentration for the full model. Quantitatively, the results are only slightly different. This can be explained by the fact that, in the full model we have a shrinking compartment, thus, as a MT shortens, GDP-tubulin remains in the shrinking compartment for some period of time before going to the GDP-tubulin compartment. Also, our shrinking compartment has a term for "rescue", where some of the MTs

that are shrinking enter back into the growing compartment.

Acknowledgments. *The program is funded thanks to the support of the A*MIDEX project (n° ANR-11-IDEX-0001-02) funded by the "Investissements d'Avenir" French Government program, managed by the French National Research Agency (ANR), and the support INSERM Plan cancer n° PC201418. D.W. was supported by the programs cited above through a post-doc funding, F.H. and M.T. were partially supported by the programs cited above. We thank Saulo de Matos Silva for his careful reading and comments, in particular for a significant improvement of proofs in Section* **??**. *We thank the anonymous referees the helpful suggestions.*

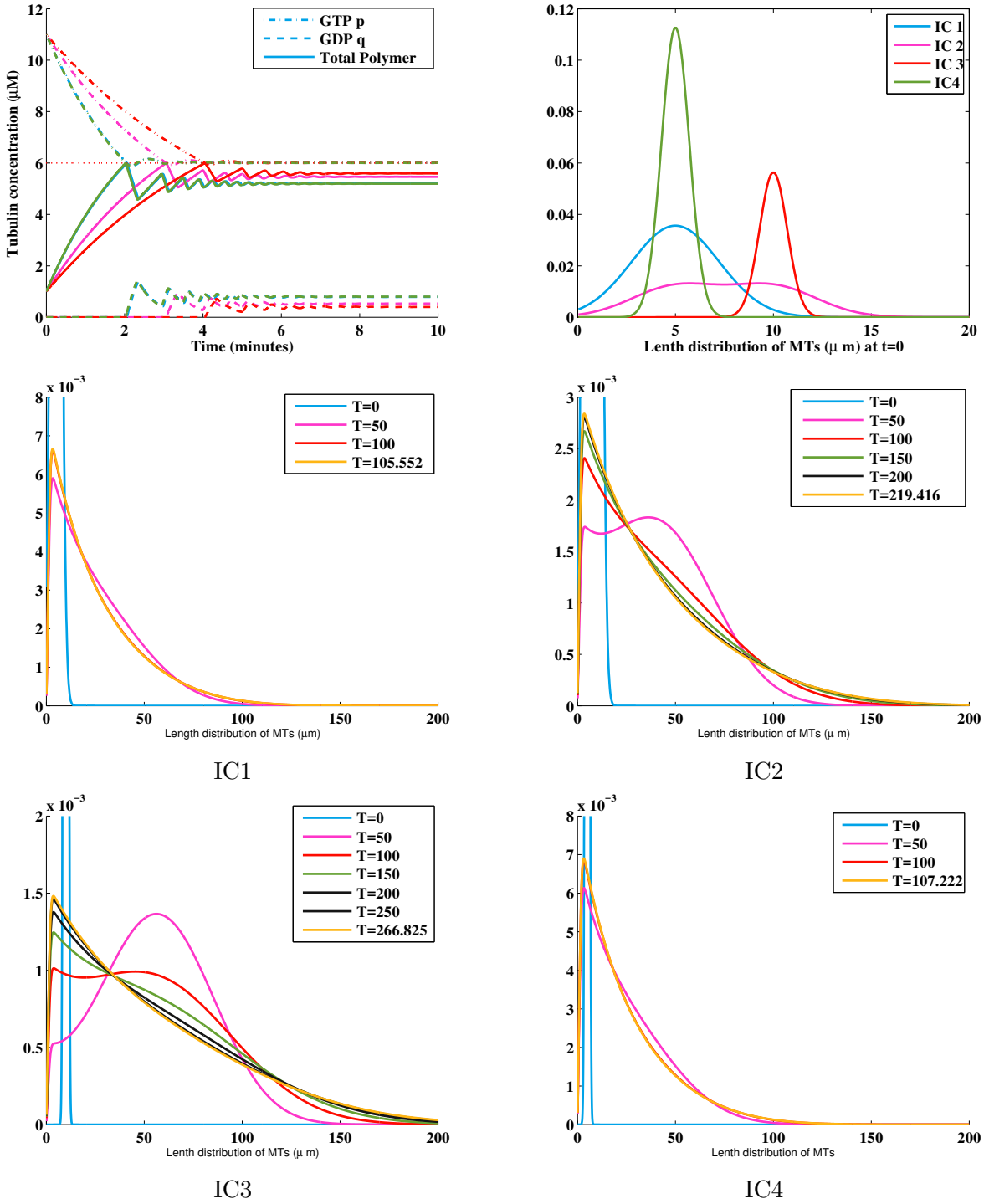

Figure 8: Upper left: Time evolution of the macroscopic quantities $p(t), q(t)$ and the mass $\int_{\mathbb{R}^+} xu(x,t)dx$ for different initial size distributions u_0, IC1: cyan, IC2: pink, IC3: red and IC4: green. Upper right: Four different initial size distributions u_0. On the four other plots are drawn the time evolution of the size distribution u until it reaches equilibrium.

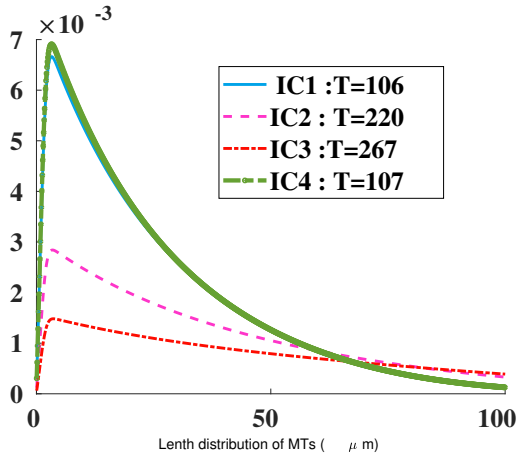

Figure 9: Asymptotic size distribution for the microtubules, for different initial size distributions u_0.

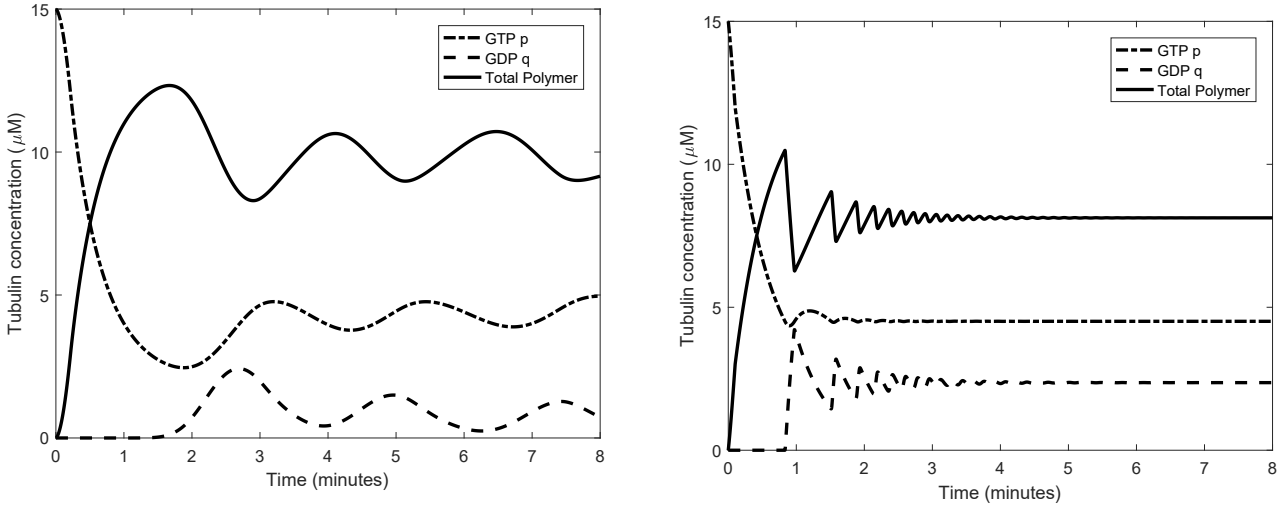

Figure 10: Left: Full model results from simulation of model in [31]. Parameters are: $\alpha = 2$, $\gamma^h = 5$, $\beta_\infty = 20$, $x_0 = 4$, $\mu = 5.9 \times 10^3$, $m = 2$, $x_{min} = 0.5$, $\kappa = 2$, $p_c = 2$, $p_N = 12$, $p_0 = 15$, $\lambda = 0.136$. Right: Simplified model of this paper. Parameters are (units given in Table 1): $\alpha = 2$, $\gamma^h = 5$, $\beta_\infty = 20$, $x_0 = 2$, $\mu = 0.1$, $m = 2$, $x_{min} = 0.8$, $\kappa = 2$, $p_c = 2$, $p_N = 12$, $p_0 = 15$.